

Geochemical investigation of NaCl-KCl-MgCl₂-CaCl₂-FeCl₂ solutions in Zechstein 2 salt, Suldrup Dome, Denmark

Microthermometry on fluid inclusions in halite

BY
JOHANNES FABRICIUS



Geochemical investigation of NaCl-KCl-MgCl₂-CaCl₂-FeCl₂ solutions in Zechstein 2 salt, Suldrup Dome, Denmark

Microthermometry on fluid inclusions in halite

BY
JOHANNES FABRICIUS

Key words:

Fluid inclusions, halite, bischofite,
P-T conditions, salt domes.

Vignette:

Fluid inclusion with bischofite and
vapour bubble in halite.

DGU Serie A nr. 27

ISBN 87-88640-46-9

ISSN 0901-0270

Oplag: 1000

Tryk: AiO Tryk as, Odense

Tegning: Eva Melskens

Dato: 3-10-1989

Johannes Fabricius,

DGU, Thoravej 8,

DK-2400 København NV

Redaktion: Leif Banke Rasmussen

© Danmarks Geologiske Undersøgelse

Thoravej 8, DK-2400 København NV

I kommission hos: Geografforlaget ApS.

Ekspedition: Fruerhøjvej 43, 5464 Brenderup

Telefon: 64 44 16 83

Contents

| | | | |
|--|----|--|----|
| Abstract | 4 | Sylvite | 13 |
| Introduction | 5 | Carnallite | 13 |
| Geological setting | 6 | Microthermometry of fluid inclusions | 13 |
| Materials and methods | 8 | Phase diagram of the system KCl-MgCl ₂ -H ₂ O .. | 13 |
| Materials | 8 | Chemical composition, cryometry | 13 |
| Materials, 1001 m level | 8 | Formation temperature, thermometry | 15 |
| Preparation of samples | 8 | Formation pressure | 15 |
| Materials, 1002 m level | 8 | Observations of cooling | 15 |
| Materials, 954 m level | 8 | Dissolving temperatures of bischofite | 17 |
| Methods | 9 | 1001 m level | 17 |
| Microthermometry | 9 | 1002 m level | 17 |
| Dissolution tests, compressed gas | 9 | Temperatures of homogenization | 19 |
| Evidence of internal stress in the test samples .. | 9 | Discussion of results | 20 |
| Fluid inclusions in halite | 10 | Fluid inclusions in halite | 20 |
| Chemical analysis of inclusion fluids | 10 | The system KCl-MgCl ₂ -FeCl ₂ -H ₂ O as model for | |
| Types of inclusions | 10 | the inclusion fluids in halite | 20 |
| Solid inclusions | 10 | Concentrated sea water, NaCl facies | 20 |
| Anhydrite, CaSO ₄ | 10 | Density and viscosity of the equilibrium | |
| Hexagonal pyrrhotite, Fe _{1-x} S | 11 | solution | 20 |
| Hematite, Fe ₂ O ₃ | 11 | Origin of KCl-MgCl ₂ -FeCl ₂ brine | 21 |
| Manganese oxide or goethite | 12 | Iron minerals | 22 |
| Clayey material | 12 | Hematite, Fe ₂ O ₃ | 22 |
| Orange yellow balls | 12 | Rinneite, 3KCl · NaCl · FeCl ₂ | 22 |
| Fluid inclusions | 12 | Pyrrhotite, Fe _{1-x} S | 22 |
| Regular inclusions | 12 | Brine mixing, salting out | 23 |
| Irregular inclusions | 12 | Temperatures and pressures of formation | 23 |
| Identification of daughter minerals | 12 | Conclusions | 25 |
| Bischofite | 12 | Acknowledgements | 26 |
| Crystallographic and optic identifikation | 12 | References | 26 |
| Melting test | 12 | | |

Abstract

Large, irregular fluid inclusions with daughter bischofite, $\text{MgCl}_2 \cdot 6\text{H}_2\text{O}$, in recrystallized halite from former brine pockets in grey Zechstein 2 rock salt from the Suldrup dome, Denmark, were studied by means of microthermometry. The test material consists of ca 3 kg cleavage pieces and a piece of core of extremely clean, colourless, limpid halite. Anhydrite and pyrrhotite are present as solid inclusions in trace amounts only. The irregular inclusions studied all contain daughter bischofite at room temperature. Optical, crystallographic, and chemical (melting) methods proved the daughter mineral to be bischofite.

The mean dissolving temperature $\bar{T}_{\text{mhex}} = 56.5 \pm 0.9^\circ\text{C}$, 95% confidence limit, of 117 measurements yields, from pertinent phase diagrams, a quantitative composition of the equilibrium solution: 114 mol $\text{MgCl}_2 + 1.2$ mol K_2Cl_2 per 1000 mol H_2O , saturated with NaCl (ca. 2 mol $\text{Na}_2\text{Cl}_2/1000$ mol H_2O). Exposed to the atmosphere, the equilibrium solution becomes orange yellowish after some days, thus proving the presence of FeCl_2 (5–10 mol/1000 mol H_2O). In one inclusion carnallite ($\text{KMgCl}_3 \cdot 6\text{H}_2\text{O}$) was observed, the dissolving temperature $T_{\text{mcar}} = 81.9^\circ\text{C}$ of which is a

minimum trapping temperature. The minimum trapping pressure is calculated at slightly higher than 65 MPa. The viscosity at 80°C is estimated at ca. 4 centipoise. Measurements of the homogenization temperature in fluid phase are meaningless due to the presence of compressed gas, possibly H_2S .

The following model is proposed concerning the formation of the studied halite:

During the end of the diapiric penetration phase in Lower Cretaceous, a metamorphic lye mixed with concentrated sea water in NaCl facies in brine pockets within the grey Zechstein 2 rock salt, causing salting out of the studied halite. The metamorphic lye derived from a metamorphosed carnallitic potash zone. The carnallitic solution was mixed with an infiltrating rineitic ($3\text{KCl} \cdot \text{NaCl} \cdot \text{FeCl}_2$) solution. The mixture was squeezed out from the potash zone during the diapiric penetration phase, leaving a trail of disseminated grains and fracture fillings of carnallite all the way up to the former brine pockets.

The minerals bischofite and pyrrhotite, Fe_{1-x}S , are reported from Denmark for the first time.

Introduction

In 1959–61 four deep wells (potash well nos. 1–4) were drilled into the Suldrup salt dome, Jutland, Denmark, by Egnsudviklingsrådets Boreudvalg, (The Drilling Committee of the Regional Development Council), a committee appointed by the Ministry of Labour. The purpose of the drilling program was to extend the knowledge of the quality and the amount of the potash salts present in the dome.

The results of the potash drillings were published by Boreudvalget (1962): *Kaliboringerne ved Suldrup 1959–1961*, vol. I-III. The report comprises lithological descriptions, chemical analyses, mineralogical analyses, and determinations of the contents of potash among other items, mostly of technical description.

At the Geological Survey are stored typical core pieces, comprising approximately 10% of the cored

material, wet and dry drilling samples and the remains from chemical analyses. Many detailed mineralogic-petrographic internal reports are also filed at the Survey. All this material constitutes an excellent basis for investigations of the geochemical systems besides the temperatures and the pressures prevailing through the geologic history of the dome.

The major objects of the present work are

- i. A thorough description of the geochemical system Na-K-Mg-Ca-Fe-Cl-(SO₄)-H₂O.
- ii. The microthermometric reactions of this system represented by fluid inclusions in halite.
- iii. The geologic aspects through time and in space of the results of the microthermometry and the rock descriptions.

Geological setting

The Danish Subbasin forms the south-eastern branch of the Northern Permian Basin (Ziegler 1981, fig. 10). During Zechstein time four evaporite cycles (Z1-Z4) precipitated in the Danish Subbasin. Fig. 1 shows the extension of the Zechstein sediments, the main dome area, and depth contours to the pre-Zechstein reflector. It can be seen that the Suldrup salt dome is situated centrally in the basin between an 8000 m and a 6000 m depth contour.

The stratigraphy of the Danish Zechstein evaporites is given in table 1 and fig. 2A. The four Zechstein cycles correspond to the North German Zechstein 1-4 cycles. The symbols used in table 1 and fig. 2 are those proposed by Richter-Bernburg (1953, p. 852) and refer to the main minerals in the layer: Na – halite, A – anhydrite, Ca – carbonate, (K) – potassic salt, K – potash zone (mainly sylvite), T – (Salz-) Ton = salt clay. The Veggerby Potash Zone K2 corresponds to the famous German Flöz Stassfurt (Richter-Bernburg 1961, p. 71).

The interpretation of the stratigraphy (table 1 and fig. 2A) is based on the works of Richter-Bernburg (1961, 1981) and Jacobsen (1984).

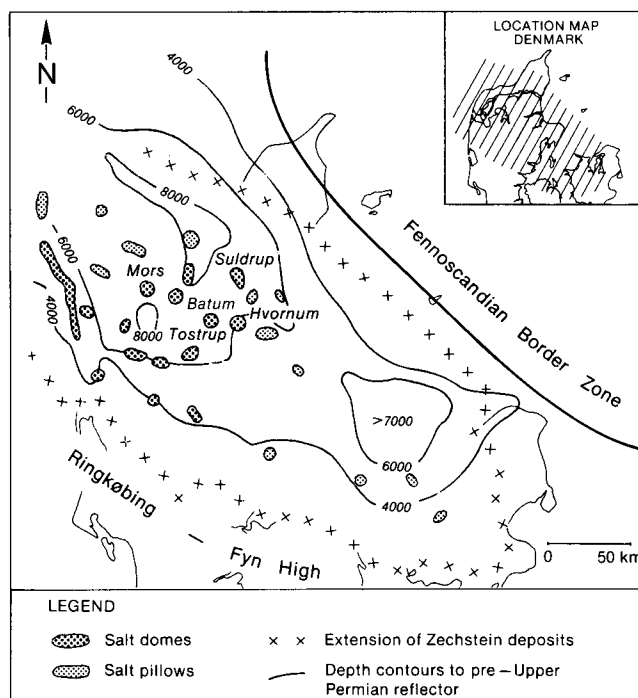


Fig. 1. Extension of the Zechstein basin with the halokinesis area. Simplified after Michelsen et al (1981).

| Cycle | Symbol | Depth m | Lithology |
|-------|--------|------------|---|
| Z4 | Na4 | 20 | rock salt, light grey to pale orange, clayey. |
| | T4 | 30-40 | salt clay, medium olive brown to olive grey to greyish black, silty clay and claystone, with rock salt. |
| Z3 | Na3 | c.100 | rock salt, red to brownish to greyish, coarse crystalline, with disseminated anhydrite and two thin potash zones and one thin bed of anhydrite. |
| | T3 | 15-60 | salt clay, sand-, silt-, claystone, red and green to greyish black, with rock salt. |
| Z2 | A2r | <1 | deck anhydrite. |
| | Na2r | 15 | deck halite, yellowish red to orange red, kieseritic, potassic, with disseminated carnallite and anhydrite, clayey. |
| | K2 | 10 | hard salt, kieserite, halite, sylvite, and anhydrite, clayey. Veggerby Potash Zone. |
| | Na2(K) | 20 | rock salt, reddish to brownish red, potassic and kieseritic. |
| | Na2 | c.600 | rock salt, light to medium grey, occ. colourless, translucent, coarse crystalline with disseminated anhydrite. |
| Z1 | Ca2 | 12-14 | anhydrite-dolomite zone, alternating layers of anhydrite, dolomite, and limestone, medium grey. |
| | A1 | 1 | anhydrite, bluish grey, compact. |
| | Na1 | c.400 | rock salt, light to medium grey, occ. colourless, translucent, coarse crystalline with disseminated anhydrite. |

Table 1. Stratigraphy of the Danish Zechstein. The Veggerby Potash Zone K2 is a kieseritic »Hartsalz« (= hard salt).

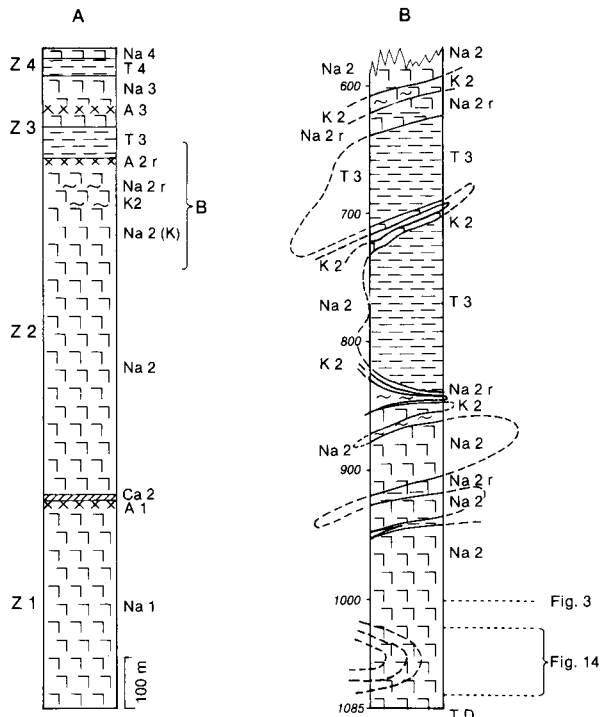


Fig. 2. A. Idealized stratigraphic column of the Danish Zechstein evaporites. Based on Richter-Bernburg (1953, 1961, 1981) and Jacobsen (1984).
 B. The lower part of the well Suldurup 15 as interpreted by Richter-Bernburg (1961).
 Abbreviations explained in Table 1.

In the well Suldurup 15 (potash well no. 2), the cap rock is found at a depth of 158 m and the salt mirror (Na₂) at drilled depth ca. 235 m. Figure 2B shows Suldurup 15 from drilled depth ca. 575 m to total depth 1085 m. It is seen that the rock types Na₂, K₂, Na₂r, and T₃ are present, whereas the coloured rock salt Na₂(K) seems to be missing. The layers are strongly folded, and the sequences are repeated and inverted in places (Richter-Bernburg 1961, app. 3).

Figure 3 shows a section of the grey Na₂ salt containing four layers of coarse grained recrystallized halite, of which the uppermost layer (1000.90–1001.40 m) and the layer 1002.00–1002.08 m will be discussed in the

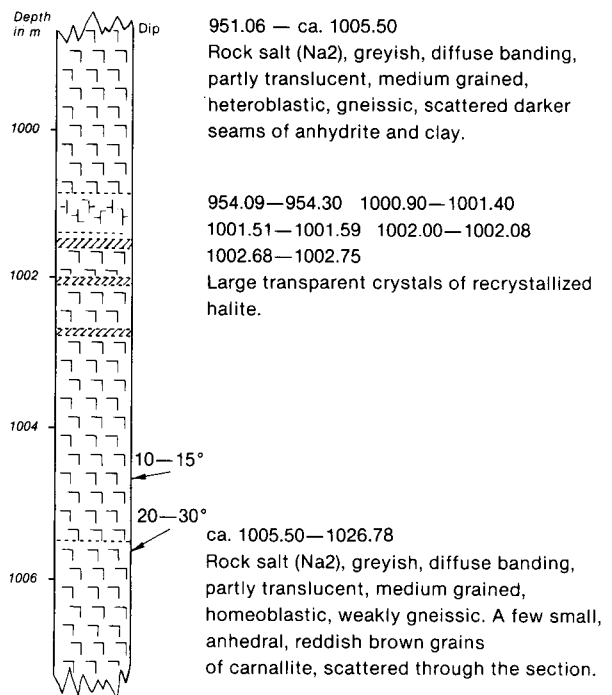


Fig. 3. Section of the grey salt Na₂ with four layers of coarse grained recrystallized halite. The layers 1000.90–1001.40 m (1001 m level) and 1002.00–1002.08 m (1002 m level) are the objects of the present work. At c. 1005.50 m supposed facies boundary. Core descriptions from Jacobsen (1961).

present work. The shown section is possibly in a normal stratigraphic position (fig. 2B), but a very weak change of facies seems to be present at a depth of ca. 1005.5 m. The core description was performed by Jacobsen (1961).

No chemical analyses of the grey Na₂ salt was carried out below 924 m drilled depth. However, an average of seven analyses of Na₂ salt from higher levels gives the following composition in weight%: CaSO₄: 1.25; MgSO₄: 0.75; KCl: 1.80; NaCl: 94.41; insoluble residue: 0.51. The rest: 1.28 comprises MgCl₂, K₂SO₄, and water of crystallization.

Materials and methods

Materials

Materials, 1001 m level

From drilled interval 1000.90–1001.40 m, approximately 3 kg of rock salt was available. The material comprises numerous cleavage pieces, some with the length of an edge up to 70 mm. The rock salt consists of large crystals of colourless, limpid halite.

Several of the larger cleavage pieces are on one side bounded by the core surface. The angle between the core axis and the crystallographic c-axis is from about 30° to about 50°. In a couple of the larger pieces, brine channels can be observed (pl. I, fig. 1). The channels follow the crystallographic directions through the salt fairly well. The cross section of the main channels is a slightly irregular rectangle measuring up to ca. 10x5 mm. Open at both ends, the channels are empty. However, ligated, closed branches and large irregular inclusions in the vicinity of the channels, besides brine, often contain numerous minute solid inclusions of anhydrite and clay

A single crystal of halite was found among the cleavage pieces: euhedral, boxlike, approximately 2.5x2.5x3 cm in size and with a dull, pitted surface (pl. I, fig. 9). The root end is a glossy cleavage face. The salt is colourless and transparent. No solid inclusions and only a few regular inclusions are observed.

Preparation of samples

After rinsing with water for drilling mud and dirt, the cleavage pieces were inspected under the stereoscopic microscope for usable fluid inclusions. The usable pieces were then divided into smaller cleavage pieces using a razor blade. Rough surfaces were grinded on silicon carbide paper no. 1200. Polishing was carried out on moistened cloth. Eventually, the samples were split into pieces, approximately 4x4x2 mm, suitable for the cooling-heating stage.

Materials, 1002 m level

At fig. 3 is noted five deposits of recrystallized halite (pl. III, fig. 1). These deposits probably formed layers

of brine rather than cavities or brine pockets. Besides the studied salt from the section 1000.90–1001.40 m drilled depth, a piece of core from drilled depth 1002.00–1002.30 is also still available.

The uppermost 8 cm of the piece of core consists of a layer (1–1.5 cm) of coarse crystalline transparent halite, the crystals of which are intergrown with a large single crystal of limpid and transparent halite. The lower face of the crystal is coated with a very thin wavy layer of minute crystals of anhydrite, forming the transition to medium grained, typical Na₂ greyish rock salt.

The large single crystal of halite contains numerous irregular fluid inclusions with euhedral bischofite as a daughter mineral. Some inclusions contain needlelike, birefringent crystals presumed to be goethite (like the crystal at pl. II, fig. 4 (arrow)). No brine channels are observed. A few crystals of euhedral pyrrhotite are found. This piece of recrystallized halite is similar to the studied halite, 1001 m level, except the lack of brine channels and yellow balls.

Materials, 954 m level

From the bottom of the interval 954.09–954.30 m drilled depth, a piece of core is available (pl. III, fig. 2). The height is ca. 75 mm and the diameter is 97 mm.

In the upper end, a layer of coarse grained (size up to 10 mm) colourless and transparent halite occurs. The grains are coated with a thin orange yellow layer of dry drilling mud. Here and there rusty grains, possibly of altered rinneite, are observed. A corner (ca. 40x30x30 mm) of a cube of halite is projecting from the coarse grained layer into the rest of the core, consisting of a large crystal of halite with the same crystallographic orientation. The surfaces of the corner are also coated with dry drilling mud. The c-axis of these crystals deviates about 30° from the core axis. No solid inclusions are visible. In parts of the piece, populations of highly irregular large fluid inclusions are observed. A very thin greyish layer of minute euhedral crystals of anhydrite is found at the lower surface of the piece of core.

Methods

Microthermometry

A ChaixMeca microthermometry apparatus, 1980 model, was used. The heating-freezing stage is commanded by an electronic manual/automatic controller and temperature read-out.

As the temperature coefficient of solubility of bischofite is as high as 0.2 (Borisenko 1978, table 2), the heating rate was held at ca. 0.1°C/min.

Dissolution tests, compressed gas

The dissolution technique was used on inclusions with and without daughter minerals. The samples were immersed in water and watched while a dissolution front approached the inclusion in question. The diameter of the bubble was measured before and after release of the bubble upon dissolution opening of the inclusion. The pressure p_1 within the inclusion before release of the bubble was calculated from $p_1V_1 = p_2V_2$, where $p_2 = 0.1$ MPa (~ 1 atm) and V is the volume of the bubble.

The tests yield an original internal pressure of 5–10 MPa on the basis of the observed bubble volume expansions. The accuracy is probably only $\pm 10\%$ at best (Roedder 1982, p. 111), because various unknown factors are involved; e.g., the thermal contraction ratio halite:liquid; the amount of »stretching« of the walls due to internal pressure; the expansion of the salt

caused by the external pressure relief from the original pressure to atmospheric pressure. However, the results clearly indicate that the bubbles are not liquid shrinkage vapour bubbles but consist of compressed gas of unknown composition. As pyrite is present, especially in potash zones and salt clay formations, the most likely major component of this gas is H_2S .

During dissolution of a homogeneous cleavage piece containing a single fluid inclusion with a gas bubble, but no visible joints, fissures or cleavage planes, innumerable minute bubbles ($< 2 \mu m$) developed over the advancing dissolution fronts on all the faces of the sample, like incipient boiling of water. The interpretation of this observation is that condensed gas has been bound as submicroscopic fluid inclusions in the lattice interstices, where the lattice is disordered or where it has vacancies (Müller and Heymel 1956, p. 315; Baar 1958, p. 145; Giesel 1968, p. 103). No indications of CO_2 gas observed during freezing runs.

Evidence of internal stress in the test samples

Stress birefringence bands (photoelastic lamellae, glide bands) in halite are due to internal stress from arrays of like-sign edge dislocations locked in the slip planes. (Carter and Heard 1970, p. 215).

Pl. I, fig. 4 shows the photoelastic lamellae in a cleavage piece of the studied halite. The lamellae are inclined at 45° to crossed polarizers. The photoelastic lamellae prove that the studied salt is stressed.

Fluid inclusions in halite

Chemical analysis of inclusion fluids

During sample preparation, a large planar, dendritic inclusion was opened (pl I, fig. 2). With a flattened cannula, 7.9 mg brine was extracted from the inclusion. The brine was diluted to 10.0 ml and analyzed by means of atomic absorption (T. Laier, pers. com. 1988). The concentrations of Mg, Na, K, and Ca in this solution were 50, 7.6, 13.3, and 2.8 mg/l, respectively. The concentrations were calculated to 63 mol $MgCl_2$, 5 mol Na_2Cl_2 , 5 mol K_2Cl_2 , and 2 mol $CaCl_2$ per 1000 mol H_2O in the original brine. The salinity is approximately 35 weight% at room temperature. The analysis agrees fairly well with the measurements of Pabalan and Pitzer (1987). The diagram fig. 4 is a recalculation from molality to mol/1000 mol H_2O of their figure 16.

After some days, during which the sample was exposed to the atmosphere, the remaining brine in the inclusion became light orange yellow, proving the presence of $FeCl_2$ in the brine (Harbort 1915, p. 250; Braitsch 1962, p. 173).

The concentration of $MgSO_4$ may be up to ca. 15 mol per 1000 mol H_2O (fig. 5) for the measured concentration of $MgCl_2$. However, as the original concentration

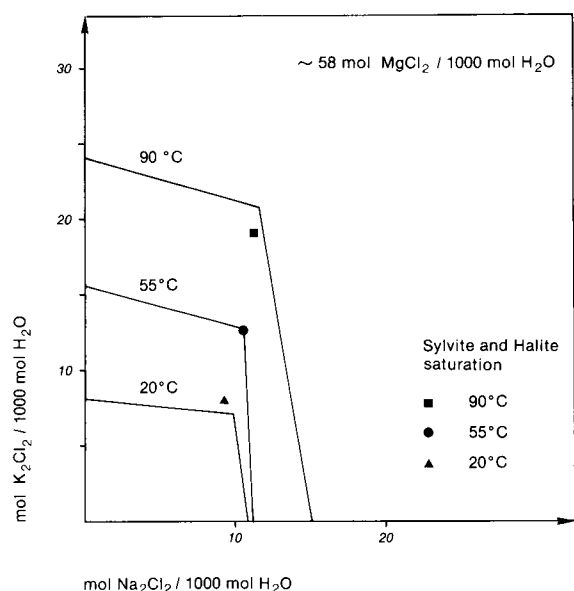


Fig. 4. Solubilities of halite and/or sylvite in the quaternary system $NaCl - KCl - MgCl_2 - H_2O$ at different temperatures and for a fixed concentration of $MgCl_2$ equal to 58 mol $MgCl_2/1000$ mol H_2O . Recalculated from data in Pabalan and Pitzer (1987, fig. 16).

of $MgCl_2$ was higher than 100 mol per 1000 mol H_2O (fig. 10), the concentration of $MgSO_4$ is less than 2 mol. According to Sonnenfeld (1984, p. 207), Azizov (1979) notes that bischofite cannot precipitate, unless the $MgCl_2$ solution is totally devoid of sulfate ions. So, the concentration of sulfate in the studied solutions may be

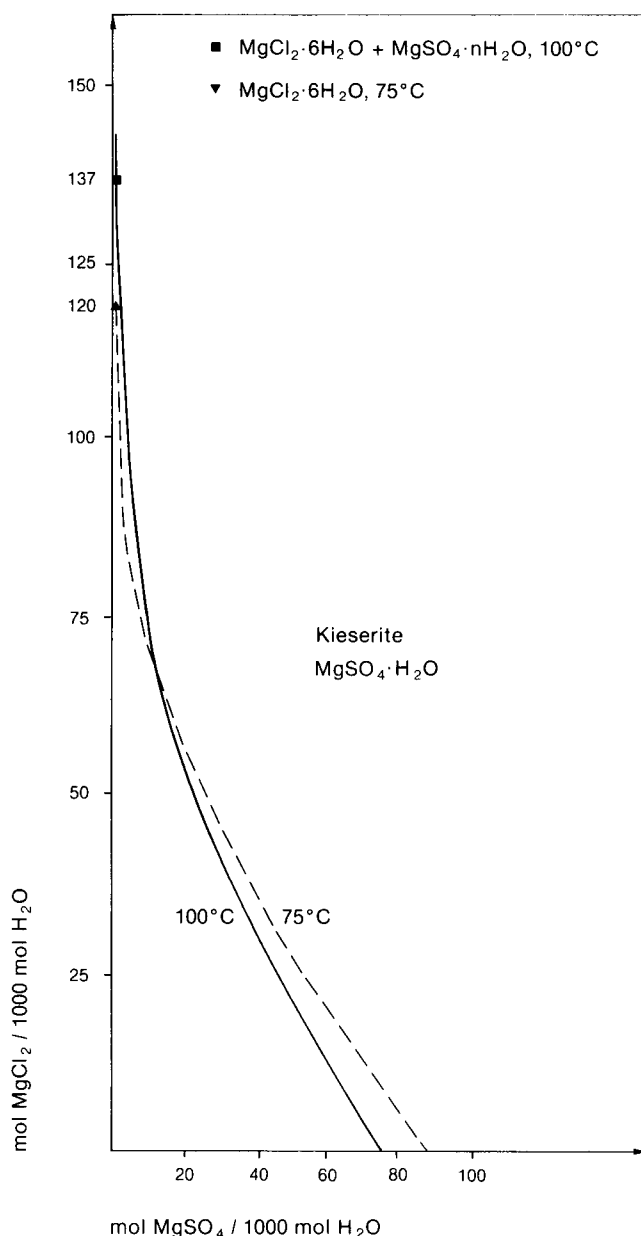


Fig. 5. Solubilities of kieserite in the system $MgCl_2 - MgSO_4 - H_2O$ at 75 and 100°C. Recalculated from data in Pabalan and Pitzer (1987, fig. 11).

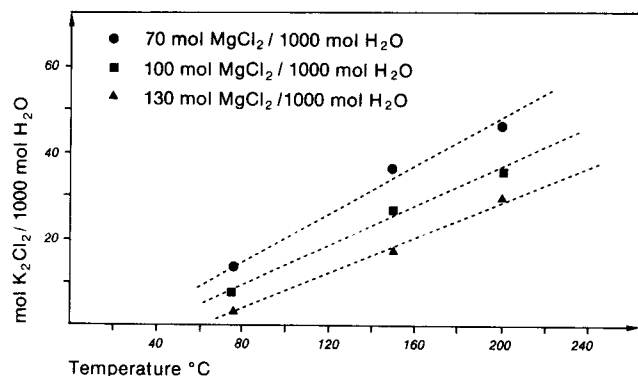


Fig. 6. KCl solubility polytherms at various fixed $MgCl_2$ concentrations. Recalculated and rearranged after Pabalan and Pitzer (1987, fig. 12).

as low as zero. In agreement with this, kieserite, $MgSO_4 \cdot H_2O$, was not observed in the salt.

The solubility of KCl in pure water is linearly dependent on the temperature (Sarig et al. 1978, p. 664). This also seems to be the case with $MgCl_2$ solutions. Solubility decreases with increasing concentration of $MgCl_2$ (fig. 6). The diagram is a recalculation and rearrangement of Pabalan and Pitzer (1987, fig. 12).

In the pure $NaCl-MgCl_2-H_2O$ system (Luznaja and Verescetina 1946, fig. 2), 63 mol $MgCl_2$ and 10 mol $NaCl$ per 1000 mol H_2O represent 24.4 and 2.4 weight%, respectively. The analysis plots practically on the phase boundary $MgCl_2 \cdot 12H_2O-NaCl$ close to the peritectic point at $-26^\circ C$ (fig. 7). The addition of KCl to this mixture causes relatively little additional drop in this invariant temperature (Roedder 1984, p. 429). Table 2 gives the eutectic temperature: $-37.8^\circ C$ for $MgCl_2-KCl$ solutions.

Consequently, the formation temperature of dodecahydrate during freezing runs on inclusions of this study will be found in the interval ca. -35 – $-25^\circ C$.

Types of inclusions

Solid inclusions

The salt is extremely clean. Solid inclusions are observed as traces only.

Anhydrite, $CaSO_4$

Sub- to euhedral orthorhombic crystals, often with the characteristically fluted prism faces. The size is from less than $50 \mu m$ to about 0.8 mm. Anhydrite is found as irregular »clouds« in the halite or on the surfaces of accidentally trapped irregular or rounded grains of col-

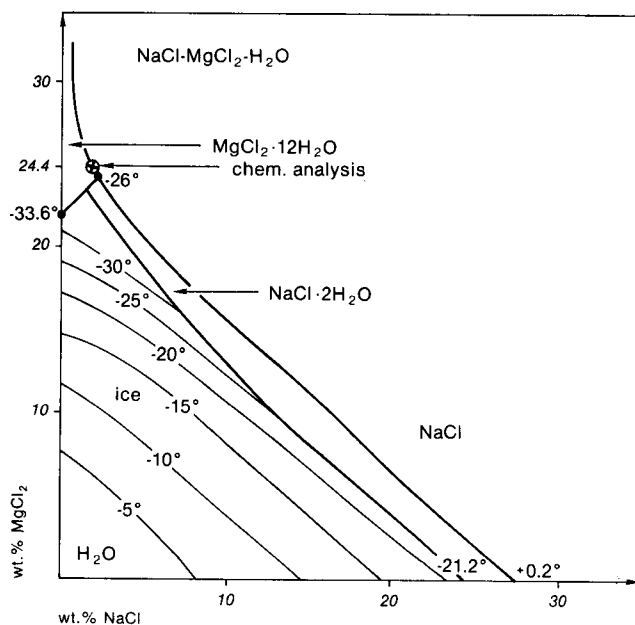


Fig. 7. Low temperature part of the phase diagram of the system $NaCl-MgCl_2-H_2O$. After Luznaja and Verescetina (1946, fig. 2).

ourless, transparent halite. No brine is present around the crystals. In a couple of instances, populations of single crystals and aggregates are trapped in large irregular fluid inclusions.

Sedimented at the bottom of the former brine pockets, a thin layer of euhedral, uncorroded minute crystals of anhydrite can be observed (pl. III, figs. 1, 2).

Hexagonal pyrrhotite, $Fe_{1-x}S$

Populations of a few hundred euhedral crystals occur on internal crystal faces of the halite, and always close to brine channels. The crystals are very thin ($2-3 \mu m$) hexagons with the length of an edge of about $20 \mu m$ up to about 0.75 mm (pl. I, figs. 3, 5). The crystals are opaque, bronze coloured with metallic lustre. The surface is either glossy, resembling thin gold foil, or dull and gritty. The crystals are magnetic, tested with a magnetic needle on separated crystals. The crystals are »dry«, except a few crystals which are surrounded by a thin film of brine.

Hematite, Fe_2O_3

In association with a few irregular fluid inclusions containing the daughter mineral bischofite, some few orange red trapezium shaped crystals were observed. The larger crystals have a longest edge of about $10 \mu m$ (pl. I, fig. 6).

Manganese oxide or goethite

In connection with a few irregular fluid inclusions (nos. 49, 52, 57, and 61), thin birefringent fibers can be observed (pl. II, fig. 4). The length of the fibers is from ca. 50 to ca. 200 μm . According to Roedder (1984), the fibers may be cryptomelane. However, because of a marked concentration of iron in the brine, the fibers may also be goethite (Wardlaw 1968, p. 1298).

Clayey material

A few inclusions show clayey material, still suspended in the brine.

Orange yellow balls

In a partly emptied narrow brine channel (pl. I, fig. 1) and in a few fluid inclusions, orange yellow balls with a diameter up to about 400 μm can be observed. The composition is unknown, but the balls may be decay products, possibly limonite (goethite), probably after rinneite (Armstrong et al. 1951, p. 684). The balls do not react upon heating up to 250°C.

Fluid inclusions

Besides artificial fluid inclusions, produced during the core drilling or the sample preparation, two types of fluid inclusions are observed:

Regular inclusions

Cube shaped inclusions with the length of an edge from less than 10 μm to about 9 μm . None of the inclusions contain daughter minerals, nor do the smaller ones contain a liquid shrinkage vapour bubble. Many of the inclusions are cubes modified by either the octahedron or both the octahedron and the dodecahedron (pl. I, fig. 8).

The regular inclusions are found as small populations on internal crystal faces or as scattered individuals, always in crystallographic orientation with the host halite. Large regular inclusions are observed in connection with the brine channels. The regular inclusions are far less abundant than the irregular.

Irregular inclusions

A large number of irregular inclusions are observed, especially in association with brine channels. In fact, some of the inclusions are ligated parts of former thin

channels (pl. I, fig. 7). Many populations consist entirely of irregular inclusions scattered through the salt, weakly orientated with the crystallography of the halite (pl. I, II).

All inclusions but two (nos. 27 and 69) contain a crystal of daughter bischofite at room temperature, and most of the inclusions also contain a vapour bubble. The liquid:vapour volumetric ratio varies from no vapour to about 1:5.

Closely associated with the populations of irregular inclusions, some few slightly irregular negative cubes are observed. Their length of an edge is from about 50 μm up to 200 μm . Each contains a daughter crystal of bischofite and often a vapour bubble.

During the sample preparation, microcracks along the crystallographic interfaces were occasionally generated, resulting in leakage from the inclusions and an increase in the volume of the vapour bubble.

Identification of daughter minerals

Bischofite

Bischofite, $\text{MgCl}_2 \cdot 6\text{H}_2\text{O}$, monoclinic, pseudo-hexagonal, $\beta = 94^\circ$, $X \parallel b$, $Y \wedge c = +9\ 1/2^\circ$, $Z \wedge a = -6^\circ$, acute bisectrix, $2V_z = 79\ 1/2^\circ$, $n_x = 1.494$, $n_y = 1.507$, $n_z = 1.528$ (Borchert and Muir 1964; Tröger 1971).

The observed bischofite is a true daughter mineral because the volumetric ratio solution:solid, expressed by the dissolving temperature, practically is the same of 117 inclusions (fig. 12) (Roedder et al. 1978, p. 7–55).

Crystallographic and optic identification

Most of the grains are euhedral crystals with a hexagonal configuration (pl. I, fig. 5; pl. II, figs. 1–4). Hydrohalite, $\text{NaCl}_2 \cdot 2\text{H}_2\text{O}$, is the only other salt mineral with a hexagonal configuration.

A separated hexagonal crystal (length: ca. 0.4 mm) from an opened inclusion was crushed on an object glass. With p-Cymene ($n = 1.4909$ at 20°C) as index liquid, the crystal pieces were examined under the microscope. On oblique B_1 cuts were measured the optic axial angle $2V > 75^\circ$, optically positive, n_x , ~ 1.4909 .

Melting test

Inclusion no. 15, close to the surface of the test sample, decrepitated after homogenization into the fluid phase at $T = 168.1^\circ\text{C}$, whereby numerous droplets were thrown out from the vent to the surface of the sample (pl. II, figs. 5–8). During the subsequent cooling, sup-

posed bischofite microlites crystallized in the droplets due to an increase in MgCl_2 concentration following a certain degree of evaporation.

One of the microlites (rectangular, $40 \times 55 \mu\text{m}$) was studied during a heating run under atmospheric pressure. In the interval $50\text{--}60^\circ\text{C}$, a small amount of water was released from the microlite and small apophyses formed along its rim. The microlite began melting in its own water of crystallization (Haug 1933, p. 16) at about 110°C and was totally melted slightly above 115°C , leaving microlites along its rim. The supposed bischofite microlite partly recrystallized at ca. 95°C during a subsequent cooling and was totally recrystallized to a crystal mush at 30°C .

Grube and Bräuning (1938, p. 138, fig. 4) measured the vapour pressure of dry, pure bischofite, sealed in evacuated glass flasks. The measurements were carried out from 20°C (3.4 mm Hg) to 160°C (744.5 mm Hg). Below 55°C (7.2 mm Hg), the process



and between 55 and 117°C (176.6 mm Hg) the process



control the vapour pressure. During slow cooling of the melt from 160°C , no crystallization of bischofite takes place when passing 117°C . The melt is metastable between 117 and 98.5°C , where bischofite crystallizes spontaneously, forming a wet crystal mush. Bischofite melts incongruently at 117.25°C , forming a few weight% of tetrahydrate + solution (Dietzel and Serowiy 1959).

As the studied microlite practically behaves like the bischofite of Grube and Bräuning, it is concluded that the daughter mineral actually is bischofite.

Sylvite

Sylvite, KCl, is cubic with $n = 1.490$, lower than the refractive index of halite: $n = 1.544$.

Sylvite has a very strong positive temperature coefficient of solubility, whereas halite has a very low positive temperature coefficient of solubility (Braitsch 1962, p. 33 ff).

Inclusion no. 71 contains a cube of sylvite ($8 \times 8 \times 8 \mu\text{m}$), which is identified by means of the characteristics mentioned above. The inclusion is the only one containing sylvite as a daughter mineral.

Carnallite

Carnallite, $\text{KMgCl}_3 \cdot 6\text{H}_2\text{O}$, is orthorhombic, pseudotrigonal with the refractive indices $n_x = 1.466$, $n_y = 1.475$, $n_z = 1.494$ equals n_x of bischofite.

On some crystals of bischofite, triangular or elongated hexagonal microlites are observed intergrown in the crystal faces and crystallographically orientated with the host (pl. II, figs. 9, 10). The dissolving temperature of the microlites is lower than the total dissolving temperature of the host bischofite.

The microlites are assumed to be carnallite in consequence of the chemical environment: MgCl_2 solutions with daughter bischofite and sylvite, combined with the optic characteristics.

In inclusion no. 27, a crystal of carnallite was observed. The identification is based on the chemical behaviour of the solution after freezing to -45°C , (see Observations of cooling).

Microthermometry of fluid inclusions

The primary goals of microthermometry are a quantitative determination of the composition of the solutions in the fluid inclusions and a determination of the formation temperature and pressure of the host minerals in order to elucidate the geologic history of the studied formation. For several reasons, these measurements cannot be obtained from fluid inclusions in halite.

Phase diagram of the system KCl-MgCl₂-H₂O

The phase diagram (fig. 8) is based mainly on Braitsch (1962, fig. 9, 1971, fig. 9) as corrected from d'Ans (1933). The diagram comprises a part of the KCl- MgCl_2 - H_2O system, saturated with NaCl, and under atmospheric pressure. The diagram of Braitsch is extended by means of measurements of concentrations and temperatures relating to the stability fields of magnesiumchloride hexa, octa, and dodecahydrate from Janat'eva (1946, fig. 3) (Fabricius 1984, fig. 5), Luzhnaja and Verescetina (1946, fig. 2) (fig. 7) and Strakhov (1962, fig. 117) (Fabricius 1987b, fig. 9). The shape of the octa- and dodecahydrate stability fields is estimated from Findlay (1907, fig. 20), (Fabricius 1987b, fig. 7).

The upper boundary of the stability field of bischofite against carnallite and MgCl_2 tetrahydrate is questionable, because the extension of the boundary bischofite-carnallite of Braitsch (1962) deviates markedly from the boundaries of d'Ans and Sypiena (1942, fig. 2).

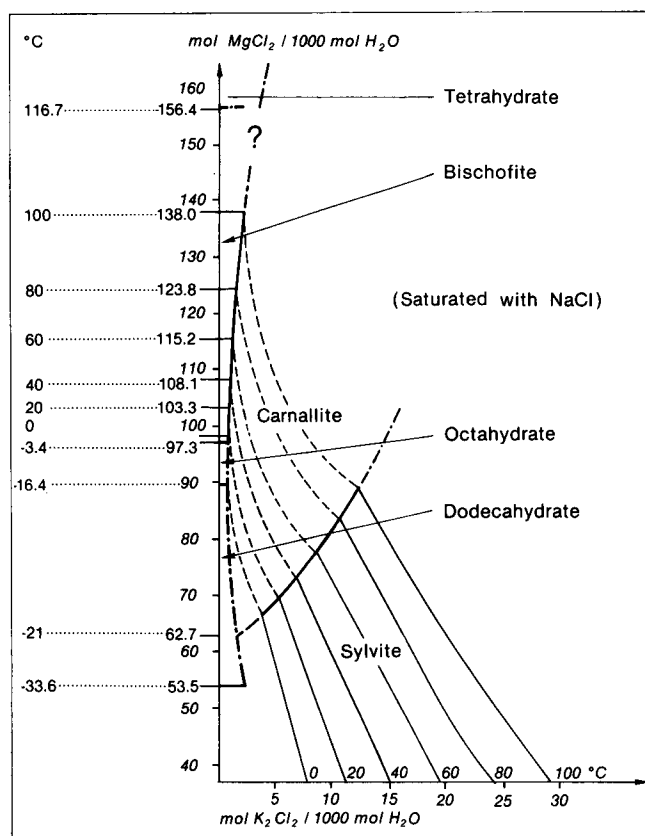


Fig. 8. Low temperature part of the phase diagram of the system $KCl-MgCl_2-H_2O$, saturated with $NaCl$. Mainly after Braitsch (1962, fig. 9). See text for further comments.

Chemical composition, cryometry

Provided the availability of pertinent phase diagrams, a semiquantitative chemical analysis of the main components of the inclusion fluid is achieved by measuring its freezing point depression. This cannot be done directly because the studied multicomponent brines are usually extremely difficult to freeze. According to Roedder (1984, p. 429), Angell and Sare (1970) observed that on cooling most of the inclusions form rigid glasses which are actually metastable supercooled liquids.

In those inclusions which form solids (ice, hydrates) after cooling down below $-100^\circ C$, the eutectic melting temperature T_e is measured on subsequent warming (table 2). However, as soon as melting of the ice takes place, the released water begins to dissolve of the wall rock ($NaCl$), forming numerous small round dissolution pits ($\varnothing 1-2 \mu m$) or dendritic grooves. These make observations of the important transformation temperatures magnesiumchloride dodeca-, octa- and hexahydrate very difficult or impossible.

In addition, due to its relatively high nucleation energy, hydrohalite ($NaCl \cdot 2H_2O$) only forms after strong supercooling (Braitsch 1962, p. 34). Hydrohalite nucleates very sluggishly between -33.6 and $-26^\circ C$ (fig. 7), making observations even more difficult. As hydrohalite also is very reluctant to melt, equilibration in order to re-establish the ceiling of the inclusion may take hours.

Finally, the humidity of the atmosphere in the laboratory causes formation of numerous Häünyian cubelets on the surface of the test sample during freezing runs, whereby observation of the inclusion is hampered. This obstacle is partly overcome by conducting a little of the exhaust nitrogen back to the test chamber through a thin nylon tube.

In order to by-pass the above mentioned difficulties, and to obtain nucleation of bischofite in the inclusions with no daughter minerals at room temperature, test samples along with silica gel were packed airtight in a plastic box. The samples were held at $-80^\circ C$ in a refrigerator for several days. Only one inclusion (no. 69) out of 43 nucleated a small grain of bischofite, indicating either a comparatively low concentration of $MgCl_2$ in the inclusion fluid or high degree of metastability. At room temperature, the resulting liquid:solid volumetric ratio was higher than 800:1.

An earlier study (Fabricius 1985, p. 248) indicates that many inclusions in halite develop planar joints parallel to the six walls of the cube shaped inclusions during freezing. These joints are caused by the excess

| Composition of salt systems | Eutectic temp. T_e °C | Phase composition, eutectic mixture |
|-----------------------------|-------------------------|--|
| $CaCl_2-NaCl-H_2O$ | -55.0 | $CaCl_2 \cdot 6H_2O + NaCl \cdot 2H_2O + ice$ |
| $CaCl_2-MgCl_2-H_2O$ | -52.2 | $CaCl_2 \cdot 6H_2O + MgCl_2 \cdot 12H_2O + ice$ |
| $MgCl_2-KCl-H_2O$ | -37.8 | $MgCl_2 \cdot 12H_2O + KCl \cdot 4H_2O + ice$ |
| $MgCl_2-NaCl-H_2O$ | -35.0 | $MgCl_2 \cdot 12H_2O + NaCl \cdot 2H_2O + ice$ |
| $NaCl-FeCl_2-H_2O$ | -37.0 | $NaCl \cdot 2H_2O + FeCl_2 \cdot 6H_2O + ice$ |
| $NaCl-KCl-H_2O$ | -23.5 | $NaCl \cdot 2H_2O + KCl \cdot 4H_2O + ice$ |
| $NaCl-H_2O$ | -21.2 | $NaCl \cdot 2H_2O + ice$ |
| $KCl-H_2O$ | -10.6 | $KCl \cdot 4H_2O + ice$ |

Table 2. Eutectic temperatures T_e °C of relevant salt systems. Extract of table 1, Borisenko (1978). As KCl never forms hydrate (Roedder 1963, p. 178), $KCl \cdot 4H_2O$ is questionable.

volume associated with the formation of ice and hydrates. After melting of the ice and hydrates, the joints are filled with minute fluid inclusions caused by the temporary overpressure of the fluid or by diffusion from the inclusion (Gerlach and Heller 1966). The inclusion has leaked, causing the formation of a larger vapour bubble and thereby a higher homogenization temperature. In consequence, homogenization measurements should be performed before cryometry measurements.

In this study, the chemical composition of the inclusion fluids is determined from the dissolving temperature T_m of the daughter bischofite present at room temperature. As the wall rock is halite, the solutions are saturated with NaCl under all experimental conditions.

Formation temperature, thermometry

Under ideal conditions the disappearance temperature T_b of the liquid shrinkage vapour bubble (i.e., homogenization into the fluid phase) can be related to the temperature of trapping of the solution (Roedder 1982, p. 111). For several reasons, however, halite is not ideal:

- i. During coring and sample preparation, microjoints connected with the inclusions may form. The inclusion may leak, whereby the volume of the bubble increases, causing a higher homogenization temperature.
- ii. The internal pressure in an inclusion increases abruptly above T_b (from ca. 10^{-3} MPa at T_b and increasing ca. 1.2 MPa/°C above T_b (Potter 1977, table 1; Roedder and Belkin 1979, p. 315; Fabricius 1988, fig. 6)). Halite becomes plastic with increasing temperature, especially in the presence of water (Gussow 1970). Roedder (1984, p., 427) suspects all T_b values above 80°C for studied bedded salt to be spurious due to stretching of the inclusion walls during the experiments. The inclusions become permanently deformed, resulting in higher T_b values.
- iii. The vapour bubbles also contain gas under pressure. Measurements of the homogenization temperature are meaningless, because the gas pressure is unknown and because the solubility of NaCl in $MgCl_2$ solutions increases with increasing temperature above 100°C (fig. 9). Because of the negative molar volume associated with halite dissolution the volume of the inclusion and therefore also the size of vapour bubble increases, resulting in higher homogenization temperature.
- iv. The partial stress relief of the salt after coring causes a certain volume increase of fluid inclusions, similarly resulting in higher homogenization temperature.

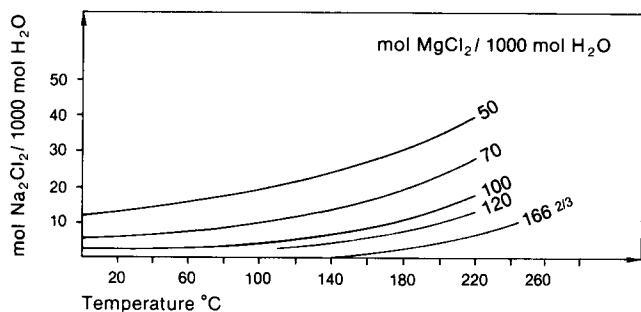


Fig. 9. NaCl solubility polytherms at various fixed $MgCl_2$ concentrations. After d'Ans and Sypiena (1942, fig. 5).

Summarizing the effects from these various factors, the larger the spread of homogenization measurements within a single crystal, the less probable that the mean homogenization temperature will have any final significance (Dreyer et al. 1949).

Formation pressure

As the temperatures of homogenization into the fluid phase are questionable or spurious, estimating the pressure prevailing during the crystallization of the studied halite cannot be based on T_b . Other methods are needed, see *Discussion of results*.

Observations of cooling

In order to check the transition temperatures between hexahydrate, octahydrate and dodecahydrate, two freezing runs were performed on inclusions containing daughter bischofite or carnallite at room temperature.

Inclusion no. 6

The sample was cooled down to -75°C, whereby the ceiling of the inclusion was covered by innumerable, very small round dissolution pits, causing a frosted, translucent, but nontransparent »window«. The sample became darker, indicating the formation of ice.

During the following warming sequence, the sample became lighter on ca. -25°C due to melting of the ice, whereby the walls became weakly transparent. Simultaneously, a faint orange yellow, blurred »shadow« became visible, possibly indicating the formation of dodecahydrate (\pm crossed nicols, gypsum plate). In the interval -21 – -18°C, nucleation of birefringent micro-lites begins from one of the corners of the inclusions. At -14°C, one third of the ceiling is covered by micro-lites. At -7°C, the ceiling is covered by a crystal mush consisting of squares, rectangles, and hexagons. At +6°C, many of the squares and rectangles dissolve. At +10°C, only hexagons were left, recrystallizing into larger crystals of bischofite. No doubt, most of the squares and rectangles were crystals of hydrohalite,

whereas the hexagons were octahydrate converting to bischofite.

Inclusion no. 27 (pl. II, figs. 11–13)

This inclusion has the highest measured concentration of MgCl_2 (table 3). It is highly probable that the crystal of carnallite is a daughter mineral like the observed microlites intergrown with the host bischofite, because no grains of carnallite is observed within the salt.

The inclusion was slowly heated until total dissolving of the carnallite (81.9°C). Its temperature coefficient of solubility (TCS) seems to be much smaller than TCS (= 0.2) of bischofite.

The inclusion was then slowly cooled down to -45°C in order to observe formation of hydrates. During the subsequent warming, numerous isotropic »stars« or »Maltese crosses« nucleated spontaneously on the ceiling of the inclusion between -45 and -35°C in crystallographic orientation with the host halite. The »Maltese crosses«, the largest of which is $70 \times 70 \mu\text{m}$, consist of cubelets of sylvite (optic identification) growing from a tetrad (quadruplets? or skeleton crystals?).

On reheating, at -20°C , a thin layer of ice formed on the upper surface of the test sample, making observations of the inclusion difficult.

At -19 – -18°C some very small anisotropic rectangular crystals nucleated in connection with the vapour bubble. The crystals are carnallite, ($\text{MgCl}_2 + \text{KCl}$), the lower stability temperature of which is -21°C (d'Ans 1933; Kühn 1952, p. 160) (fig. 8).

From -18 to -2°C , all the sylvite crystals disappear or transform to carnallite with the same cross shape. Many small anisotropic rectangles and squares form especially in the vicinity of the bubble. From -2 to $+7^\circ\text{C}$, some of the rectangles and squares disappear (maybe hydrohalite) and some re-crystallize to hexagons (possibly bischofite).

During heating to ca. 60°C , all grains of carnallite and possible bischofite except one dissolved. The sample was shock cooled to $+13^\circ\text{C}$, whereby large dendritic skeleton crystals formed from the remaining grain of carnallite.

Even a certain metastability is reflected by the noted temperatures during the runs, the temperatures are close to the transition temperatures of fig. 8, remembering that carnallite recrystallizes incongruently, i.e. sylvite has to form before the formation of carnallite (Campbell et al. 1934).

Dissolving temperatures of bischofite

1001 m level

The dissolving temperatures $T_{m,hex}$ of 69 crystals of daughter bischofite and one of carnallite (no. 27) are noted in table 3. The mean \bar{T}_m hex of 68 crystals equals $55.8^\circ\text{C} \pm 1.2^\circ\text{C}$, 95% confidence limit.

As the isotherms of the actual dissolving temperatures in the bischofite stability field of the phase diagram (fig. 8) are perpendicular to the MgCl_2 concentration axis (Braitsch 1962, fig. 9), the concentration of MgCl_2 (mol per 1000 mol H_2O) in the equilibrium solution is independent of the concentration of K_2Cl_2

and also of Na_2Cl_2 (Dietzel and Serowy 1959, p. 15). Therefore, the more accurate polytherm of Dietzel (1959), drawn at fig. 10, can be used to determine the concentration of MgCl_2 in the equilibrium solution. The concentration of MgCl_2 ranges from 110 to 117 mol with the average of 114 mol per 1000 mol H_2O , except inclusion no. 27 (124 mol) and inclusion no. 69 (108 mol). The concentration of Na_2Cl_2 on the actual dissolving temperatures and concentrations of MgCl_2 is ca. 2.0 mol per 1000 mol H_2O (fig. 9).

The concentration of K_2Cl_2 may be variable between zero and 1.2 mol per 1000 mol H_2O (fig. 8). However,

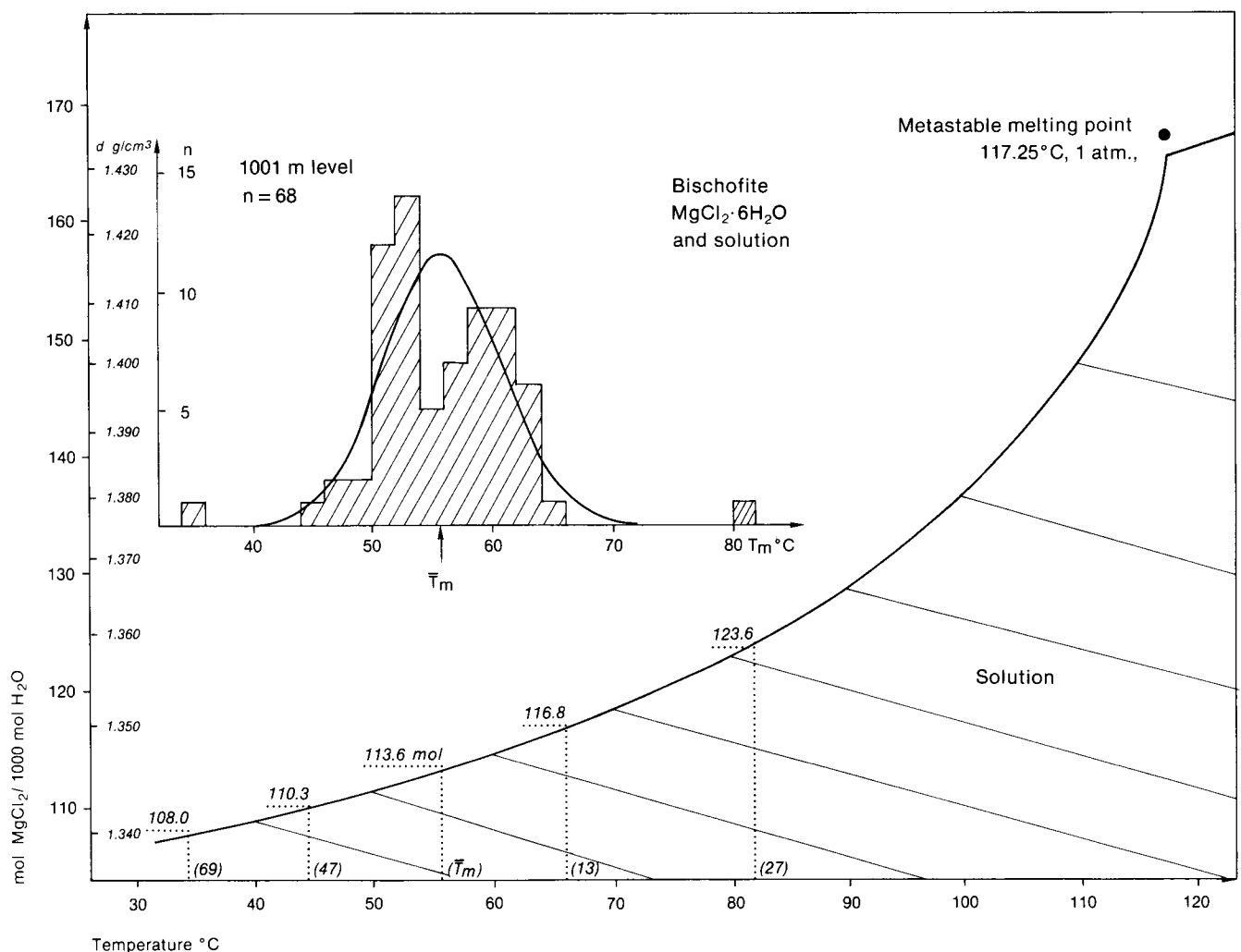


Fig. 10. Concentration and density of solutions in equilibrium with bischofite in the system $\text{MgCl}_2\text{-H}_2\text{O}$ from 30°C to the incongruent melting point of bischofite at 117.25°C , 1 atmosphere with density polytherms. After Dietzel (1959). The inset histogram comprises the measured dissolving temperatures T_m of bischofite in the 1001 m level sample. The numbers in brackets refer to inclusion numbers (table 3). The density scale is valid for pure MgCl_2 solutions.

| Sample no. | Incl. no. | T _m hex °C | mol MgCl ₂ | wt.% MgCl ₂ | Sal. wt. % | Mean T _m °C |
|------------|-----------|-----------------------|-----------------------|------------------------|------------|------------------------|
| 1 | 1 | 52.5 | 113 | 36.9 | 38.3 | 51.8 |
| | 2 | 51.0 | 112 | 36.7 | 38.1 | |
| 2 | 3 | 56.5 | 114 | 37.1 | 38.5 | 51.3 |
| | 4 | 46.9 | 110 | 36.3 | 37.7 | |
| | 5 | 50.5 | 112 | 36.7 | 38.1 | |
| 3 | 6 | 58.4 | 115 | 37.3 | 38.7 | 53.8 |
| | 7 | 59.3 | 115 | 37.3 | 38.7 | |
| | 8 | 51.5 | 112 | 36.7 | 38.1 | |
| | 9 | 50.4 | 112 | 36.7 | 38.1 | |
| | 10 | 49.5 | 111 | 36.5 | 37.9 | |
| 4 | 11 | 51.1 | 112 | 36.7 | 38.1 | 53.9 |
| | 12 | 56.6 | 114 | 37.1 | 38.5 | |
| 5 | 13 | 66.0 | 116 | 37.5 | 38.9 | 66.0 |
| 6 | 14 | 61.0 | 115 | 37.3 | 38.7 | 61.4 |
| | 15 | 61.7 | 115 | 37.3 | 38.7 | |
| 7 | 16 | 60.2 | 115 | 37.3 | 38.7 | 60.2 |
| 8 | 17 | 62.8 | 116 | 37.5 | 38.9 | 61.6 |
| | 18 | 61.3 | 115 | 37.3 | 38.7 | |
| | 19 | 61.4 | 115 | 37.3 | 38.7 | |
| | 20 | 62.8 | 116 | 37.5 | 38.9 | |
| | 21 | 60.4 | 115 | 37.3 | 38.7 | |
| | 22 | 63.3 | 116 | 37.5 | 38.9 | |
| | 23 | 61.3 | 115 | 37.3 | 38.7 | |
| | 24 | 63.7 | 116 | 37.5 | 38.9 | |
| | 25 | 59.7 | 115 | 37.3 | 38.7 | |
| | 26 | 59.4 | 115 | 37.3 | 38.7 | |
| 10 | 27 | 81.9 | 124 | 39.1 | 40.5 | (-) 61.4 |
| | 28 | 63.9 | 116 | 37.5 | 38.9 | |
| | 29 | 61.9 | 115 | 37.3 | 38.7 | |
| | 30 | 58.4 | 115 | 37.3 | 38.7 | |
| 11 | 31 | 61.1 | 115 | 37.3 | 38.7 | 59.4 |
| | 32 | 63.5 | 116 | 37.5 | 38.9 | |
| | 33 | 57.5 | 114 | 37.1 | 38.5 | |
| | 34 | 57.9 | 114 | 37.1 | 38.5 | |
| | 35 | 59.4 | 115 | 37.3 | 38.7 | |
| | 36 | 59.4 | 115 | 37.3 | 38.7 | |
| | 37 | 60.0 | 115 | 37.3 | 38.7 | |
| | 38 | 56.9 | 114 | 37.1 | 38.5 | |
| | 39 | 57.8 | 114 | 37.1 | 38.5 | |
| | 13 | 40 | 54.5 | 113 | 36.9 | |
| 41 | | 48.0 | 111 | 36.5 | 37.9 | |
| 42 | | 52.3 | 113 | 36.9 | 38.3 | |
| 43 | | 52.1 | 113 | 36.9 | 38.3 | |
| 44 | | 52.4 | 113 | 36.9 | 38.3 | |
| 45 | | 51.0 | 112 | 36.7 | 38.1 | |
| 46 | | 50.9 | 112 | 36.7 | 38.1 | |
| 47 | | 44.4 | 110 | 36.3 | 37.7 | |
| 14 | 48 | 53.4 | 113 | 36.9 | 38.3 | 52.3 |
| | 49 | 51.1 | 112 | 36.7 | 38.1 | |
| 15 | 50 | 55.2 | 113 | 36.9 | 38.3 | 53.6 |
| | 51 | 53.4 | 113 | 36.9 | 38.3 | |
| | 52 | 52.9 | 113 | 36.9 | 38.3 | |
| | 53 | 52.7 | 113 | 36.9 | 38.3 | |
| 16 | 54 | 53.3 | 113 | 36.9 | 38.3 | 53.1 |
| | 55 | 52.8 | 113 | 36.9 | 38.3 | |
| | 56 | 54.1 | 113 | 36.9 | 38.3 | |
| | 57 | 55.2 | 113 | 36.9 | 38.3 | |
| | 58 | 54.5 | 113 | 36.9 | 38.3 | |
| | 59 | 51.5 | 112 | 36.7 | 38.1 | |
| | 60 | 51.5 | 112 | 36.7 | 38.1 | |
| | 61 | 56.3 | 114 | 37.1 | 38.5 | |
| | 62 | 52.3 | 113 | 36.9 | 38.3 | |
| | 63 | 52.2 | 113 | 36.9 | 38.3 | |
| | 64 | 51.5 | 112 | 36.7 | 38.1 | |
| | 65 | 51.4 | 112 | 36.7 | 38.1 | |
| | 19 | 66 | 52.7 | 113 | 36.9 | |
| 67 | | 52.9 | 113 | 36.9 | 38.3 | |
| 21 | 68.1 | 49.4 | 111 | 36.5 | 37.9 | 54.2 |
| | 68.2 | 58.9 | 115 | 37.3 | 38.7 | |
| 22 | 69 | 34.3 | 108 | 35.8 | 37.2 | 34.3 |

T_m hex = 55.8 ± 1.2°C, 95% confidence limit. n = 68, inclusion nos. 27 and 69 excluded.

Table 3. Measured and calculated data. T_m hex: dissolving temperature of daughter bischofite. mol MgCl₂: mol/1000 mol H₂O. Sal. wt.%: salinity (weight%) including 0.6 wt.% KCl and 0.8 wt.% NaCl. Inclusion no 27 contains daughter carnallite, not bischofite.

inclusion no. 71 contained a cube of sylvite as the sole daughter mineral, the dissolving temperature of which was 40.4°C, combined with the presence of carnallite in inclusion no. 27, thus indicating a concentration of K_2Cl_2 of 1.2 mol per 1000 mol H_2O .

Inclusion no. 71 is observed in sample no. 19 in a row between inclusion no. 66 and no. 67, having a concentration of 113 mol $MgCl_2$ per 1000 mol H_2O (table 3). As sylvite is the only daughter mineral, the concentration is maximum 72.5 mol $MgCl_2$ per 1000 mol H_2O (fig. 8), i.e., the intersection point between the 40°C isotherm and the boundary between the sylvite and carnallite stability fields. In this point, the K_2Cl_2 concentration is 6.5 mol per 1000 mol H_2O . The solution is saturated with NaCl: ca. 2.5 mol Na_2Cl_2 per 1000 mol H_2O under these conditions (Braitsch 1962 fig. 11).

As the concentrations of $MgCl_2$ vary by only 7 mol per 1000 mol H_2O (inclusions nos. 27 and 69 not included), the concentrations of KCl and NaCl represent 0.6 and 0.8 weight%, respectively. The concentrations of $MgCl_2$ in mol per 1000 mol H_2O and in weight% are noted in table 3, along with the salinity of the equilibrium solution, ignoring the minor concentrations of $CaCl_2$, $FeCl_2$ and $MgSO_4$ etc. The mean dissolving temperature for each sample is also noted.

On fig. 10, the histogram of the $T_{m,hex}$ measurements is combined with the polytherm of the equilibrium solution of the pure $MgCl_2 - H_2O$ system up to the metastable melting point of bischofite (Dietzel 1959, fig. 2 and app. 1). The density scale refers to the density (g/cm^3) of the pure $MgCl_2$ solution.

1002 m level

The dissolving temperature $T_{m,hex}$ of daughter bischofite was measured on 49 irregular fluid inclusions in recrystallized halite from the interval 1002.00 – 1002.30 m drilled depth.

The measurements are shown in the histogram fig. 11. The mean $\bar{T}_{m,hex} = 57.5 \pm 1.5^\circ C$, 95% confidence limit, corresponds to 114.0 mol $MgCl_2$ per 1000 mol H_2O (fig. 10).

The histogram fig. 12 demonstrates the sum of the measurements from the 1001 m level (fig. 10) and the 1002 m level (fig. 11). The mean $\bar{T}_{m,hex} = 56.5 \pm 0.9^\circ C$, 95% confidence limit, corresponding to 113.8 mol $MgCl_2$ per 1000 mol H_2O .

Temperatures of homogenization

Several inclusions, especially the smaller regular ones, had not nucleated a liquid shrinkage vapour bubble due to stretched fluids. The temperatures of homogenization into the fluid phase of 27 inclusions with a bubble were measured in the interval 65–150°C. The measurements are scattered all over the interval with a mean temperature of ca. 105°C. A few inclusions homogenized above 200°C and several inclusions showed increasing bubble volume above 250°C.

No Brownian bubble movements were observed, indicating a high viscosity of the solutions (see *Discussion of results*).

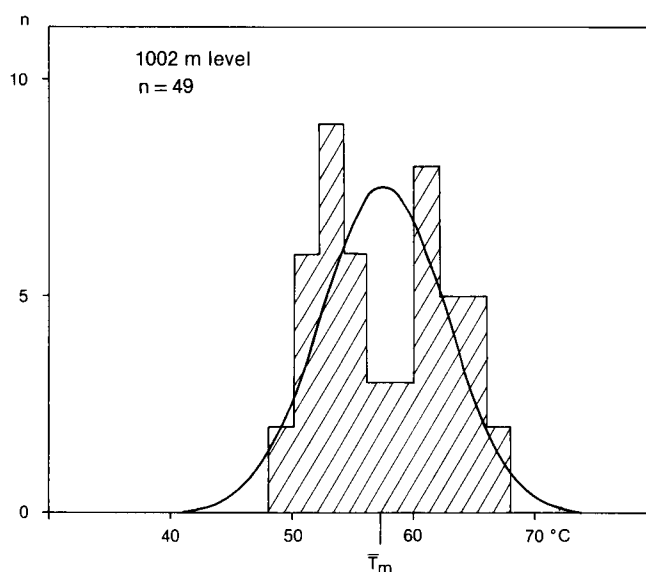


Fig. 11. Histogram of dissolving temperatures $T_{m,hex}$ of bischofite in inclusions from the 1002 m level. The mean $T_{m,hex} = 57.5 \pm 1.5^\circ C$, 95% confidence limit, corresponding to 114.0 mol $MgCl_2$ per 1000 mol H_2O .

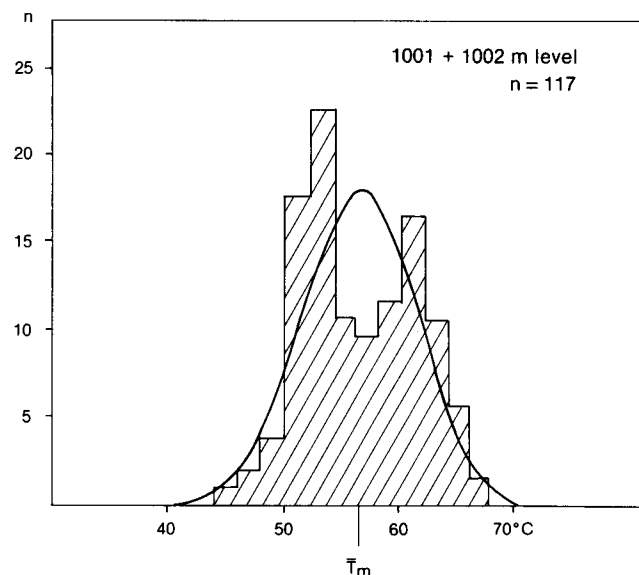


Fig. 12. Histogram of the dissolving temperatures $T_{m,hex}$ of bischofite from the 1001 m plus the 1002 m level (fig. 10 + fig. 11). The mean $T_{m,hex} = 56.5 \pm 0.9^\circ C$, 95% confidence limit, corresponding to 113.8 mol $MgCl_2$ per 1000 mol H_2O .

Discussion of results

Fluid inclusions in halite

Previous experience concerning microthermometry on fluid inclusions in halite (Roedder 1963, 1982, 1984; Roedder et al. 1978) shows that results can be obtained if salinity is comparatively moderate (26–28 wt.%), i.e., NaCl solutions with only minor amounts of other constituents. The vast majority of the reported inclusions are negative cubes in perfect crystallographic orientation with the host halite. Despite several problems during freezing and heating runs, such as permanently stretched walls, »stretched« fluids under negative pressure (Roedder 1967), strong supercooling and sluggish formation and melting of hydrohalite, the results are normally usable for interpreting the chemical and physical conditions of the salt formation on condition that NaCl is the major constituent.

In the present study, regular inclusions are far fewer than irregular inclusions. Concentration of MgCl_2 in solutions of the regular inclusions is $108 \leq \text{mol}/1000 \text{ mol H}_2\text{O}$, whereas irregular inclusions show $\text{mol MgCl}_2 \geq 110 \text{ mol}/1000 \text{ mol H}_2\text{O}$. There seems to be a threshold value of ca. 110 mol MgCl_2 between regular and irregular inclusions. The explanation for this difference may be that the solubility of NaCl strongly decreases with increasing concentration of MgCl_2 (fig. 9), so that the irregular inclusion therefore cannot be fully modified in the direction of lowest possible energy level, i.e., bounded by crystal planes (Tuttle 1949, p. 335; Roedder 1971, p. 332).

The inclusions deriving from ligated brine channels are strongly irregular without crystal faces, indicating a very high concentration of MgCl_2 . Zdanovskij (1949, p. 585, fig. 5) found that the solubility of NaCl at 105°C decreased dramatically from ca. 28 wt.% to very small values close to zero, when the concentration of MgCl_2 increased from zero to ca. 43 wt.%, corresponding to ca. 140 mol/1000 mol H_2O . As the daughter mineral bischofite is present in the long and slender, highly irregular ligated brine channels, the concentration of MgCl_2 may be at least 140 mol/1000 mol H_2O with corresponding dissolving temperatures of the daughter bischofite being higher than 100°C (fig. 8).

In the present study, measurements of the freezing point depression failed more or less, and the measurements of the homogenization temperatures are meaningless due to compressed gas in the inclusions. The dissolving temperatures of the daughter minerals pre-

sent at room temperature, however, give valuable information on the chemistry of the involved solutions and hence the genesis of the host halite, including minimum formation temperature and pressure.

The system $\text{KCl-MgCl}_2\text{-FeCl}_2\text{-H}_2\text{O}$ as model for the inclusion fluids in halite

Concentrated sea water, NaCl facies

The recrystallized halite from the former brine pockets (954 (pl. III, fig. 2), 1001 and 1002 m level) is extremely clean, with only traces of solid inclusions (anhydrite and pyrrhotite). However, the thin layers of euhedral minute crystals of anhydrite, sedimented at the bottom of the pockets, combined with the halite and the low concentration of CaCl_2 unambiguously indicate that the former brine is concentrated sea water in NaCl facies, i.e., the mother lye (Holser 1979, figs. 3, 13).

Density and viscosity of the equilibrium solution

The density scale of fig. 10 refers to the pure MgCl_2 solutions. With fixed concentrations of MgCl_2 , the density increases with increasing concentration of KCl. Hence, the density of the studied solutions is slightly higher than indicated on the density scale. The density of the carnallite equilibrium solution of inclusion no. 27 may be appreciably higher than the 1.36 g/cm³ indicated on the scale.

As no Brownian movements of the vapour bubble during heating runs are observed, viscosity must be high even at high temperatures. According to Karcz and Zak (1987, p. 730, fig. 8b), viscosity increases with increasing density. However, the rate of increase depends on the type of brine. Increase of viscosity at 20°C is much less for a NaCl brine than for a MgCl_2 brine having the same increase of density from 1.10 to 1.25 g/cm³. Viscosity increases from ca. 1.2 to ca. 3 centipoise (cp) for the NaCl brine but to ca. 5.8 cp for the MgCl_2 brine. A 4 m NaCl brine, having a density of 1.13 g/cm³ at 25°C, has a viscosity of 1.38 cp (Ranganathan and Hanor 1988, p. 180). (1 cp = 1×10^{-2} g/cmxs).

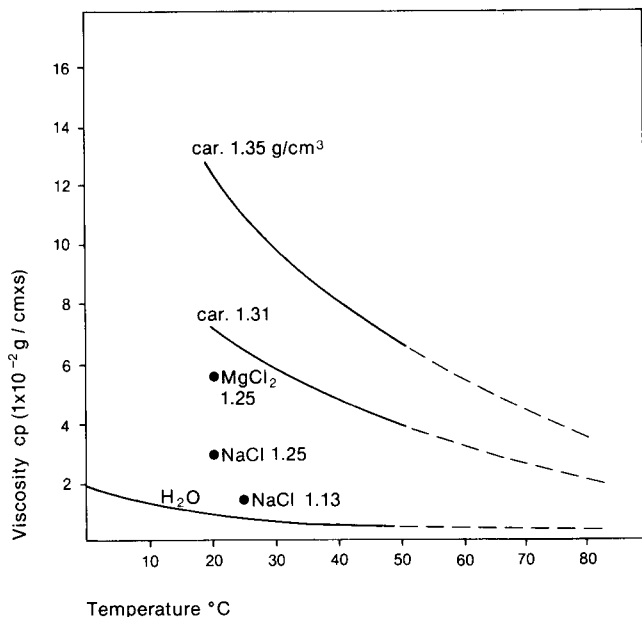


Fig. 13. Viscosity (in centipoise, cp) vs. temperature (°C) of solutions with densities (g/cm³) as indicated. Car.: carnallitic solution (MgCl₂ + KCl). Full curves after Karcz and Zak (1987, fig. 8 a,b), extrapolated (dashed curves) to 80°C.

Viscosity depends strongly on temperature (fig. 13). For a carnallitic brine with a density of 1.35 g/cm³, viscosity drops from ca. 13 cp at 20°C to ca. 6 cp at 60°C and ca. 4 cp at 80°C.

Origin of KCl-MgCl₂-FeCl₂ brine

Fig. 14 is based on the petrographic-mineralogic core descriptions of Jacobsen (1961). The section from drilled depth ca. 1025 m to ca. 1075 m is classified as Na₂ salt by Richter-Bernburg (1961) (fig. 2B). However, as the section comprises grey, coloured and black rock salt, layers of strongly tectonized anhydrite, and a thin layer of hard salt (table 1), it is postulated that, besides Na₂, Na₂(K), K₂, Na₂r, and maybe A₂r are also present (fig. 2A). The dip measurements clearly show a marked interfolding of the various rock types. The variation of the dip is pronounced around the layer of hard salt (1054.26–1054.34 m) consisting of sylvite, kieserite, carnallite, and halite. The hard salt is undoubtedly the remnant of a former potash zone K₂, probably smeared out during the diapirism.

The section (fig. 14) is mineralized with secondary carnallite above as well as below the layer of hard salt (pl. III, fig. 3). This mineralization combined with the paragenesis of the hard salt strongly indicates a progressive geothermal metamorphism of the most important primary potash salt paragenesis of ocean salt deposits: carnallite – halite – epsomite (MgSO₄ · 7H₂O)/sakiite (MgSO₄ · 6H₂O) (Kokorsch 1960, p. 62). Melting of cryophilic epsomite or sakiite triggers off the thermal metamorphism of carnallite. If the metamor-

phic lye from this stage remains in contact with the salts, the end product will be the most important metamorphic stage: carnallite – kieserite – sylvite – halite hard salt, coexisting with a metamorphic lye rich in MgCl₂ and, to a lesser extent in KCl, and being saturated with NaCl (Borchert and Muir 1964, pp. 106–7). If incongruent melting of the carnallite took place at temperatures higher than 167.5°C, the resulting solution would consist of 166.7 mol MgCl₂ + 20.85 mol K₂Cl₂ per 1000 mol H₂O, and being saturated with NaCl (Braitsch 1962, p. 87). The melting temperature of carnallite is pressure dependent after the formula $T_m = 167.5^\circ\text{C} + dT/dP(P_m - 0.1)^\circ\text{C}$, where $dT/dP = 0.1^\circ\text{C}/\text{MPa}$ above 0.1 MPa (Fabricius and Rose-Hansen 1987).

The presence of secondary rinneite (pl. III, fig. 4) in the section (fig. 14) strongly indicates an incongruent melting of carnallite combined with infiltrating solutions rich in FeCl₂ (Braitsch 1962, p. 173).

During the diapirism, the metamorphic lye is squeezed away from contact with the hard salt, whereby carnallite precipitates in the surrounding salt

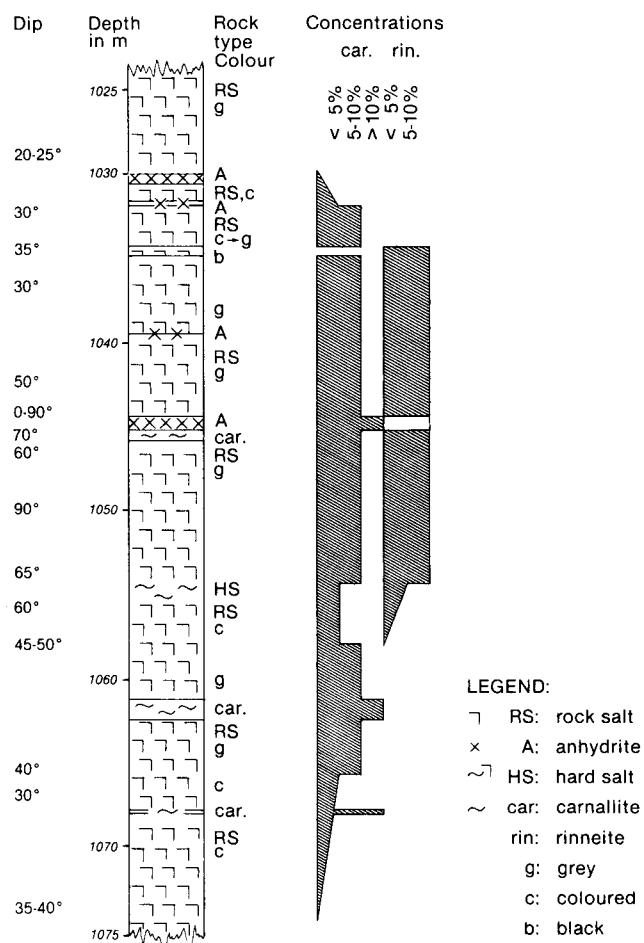


Fig. 14. Suldrup 15 from drilled depth 1025 to 1075 m based on logs (Egnsudviklingsrådets Boreudvalg 1962, vol III) and core descriptions by Jacobsen (1961). The dip measurements and the variation of rock types indicate heavy tectonic disturbances. The concentrations of secondary carnallite and rinneite are based on volumetric estimates.

in fractures and pores during later cooling. The remaining solution after the formation of carnallite will be a highly concentrated MgCl_2 brine with some KCl and FeCl_2 , and still saturated with NaCl .

Iron minerals

Sea water is deficient in iron, and the concentration of a volume of sea water up to carnallite saturation would still contain only negligible amounts of iron (Sonnenfeld 1984, p. 206). The iron present in salt deposits in the form of iron minerals or in solution originates from continental weathering solution products (Braitsch 1962, p. 171).

Hematite, Fe_2O_3

In a few of the studied inclusions, small red crystals of hematite were observed (pl. I, fig. 6). The presence of hematite unambiguously point to a primary potash deposit, preferably carnallite (Borchert and Muir 1964, p. 115). According to Harbort (1915, p. 252), Boeke (1911) demonstrated that FeCl_2 must be a widespread original constituent of the salt deposits, especially of carnallite. Boeke concluded, from the presence of hematite in carnallite and combined with the amount of FeCl_2 , that the formation of the small red flakes of hematite is caused by the FeCl_2 . Therefore, the observed crystals of hematite were transported by the bitter brine from an altered primary potash deposit, e.g., the section shown at fig. 14.

Rinneite, $3\text{KCl} \cdot \text{NaCl} \cdot \text{FeCl}_2$

The studied solutions contain a certain concentration of FeCl_2 (pl. I, fig. 2; *Chemical analysis*) as well as possible decay products after rinneite: orange yellow balls. These balls are found in brine channels and in a few fluid inclusions (pl. I, figs. 1, 5), but not as solid inclusions in the studied halite.

Rinneite is a product of secondary iron-rich solutions with no connection to the original brines. FeCl_2 somehow formed outside the potash deposit and has then, in solution, infiltrated the deposit (d'Ans and Freund 1954, p. 3).

In their classic work, d'Ans and Freund provide other models for the formation of FeCl_2 ; e.g., (p. 6), reaction of infiltrating FeSO_4 solutions with MgCl_2 solutions at 135°C , resulting in formation of kieserite and FeCl_2 in solution. In this case, the MgCl_2 solution derives from incongruent melting of carnallite at temperatures above 167.5°C . This yields a concentration of 167 mol MgCl_2 plus 21 mol K_2Cl_2 per 1000 mol H_2O , equaling a salinity of ca. 50 wt%.

D'Ans and Freund constructed the phase diagram at 55°C for the system $\text{KCl}-\text{MgCl}_2-\text{FeCl}_2-\text{H}_2\text{O}$ saturated with NaCl . They found the concentration of the equilibrium solution for the corner sylvite-rinneite-carnallite to be 4.0 mol Na_2Cl_2 , 14.0 mol K_2Cl_2 , 72.5 mol MgCl_2 , and 21.0 mol FeCl_2 per 1000 mol H_2O , which equals a salinity of ca. 40 wt%. This concentration is also valid for 83°C (figs. 2, 3, p. 4). It is not known how these concentrations may change under the influence of increasing temperature.

Rinneite decomposes into sylvite, halite, and yellow limonite (Armstrong et al. 1951, p. 685). Stewart (1951, pp. 563–7) observed in the Eskdale no. 2 boring, G.B., small rounded relics of rinneite, replaced by halite and sylvite. The diameter of the relics is ca. 100–350 μm . The orange yellow balls observed in this study probably are altered relics of rinneite transported by the infiltrating bitter brine.

Pyrrhotite, Fe_{1-x}S

Pyrrhotite occurs as delicate euhedral crystals on internal cleavage faces in the studied halite (pl. I, figs. 1, 3, 5) and accidentally trapped in a couple of fluid inclusions. The larger populations occur in the vicinity of brine channels in the same level. According to Braitsch (1962, p. 177), the crystals of pyrrhotite fulfill the demands on authigenic minerals.

Berner (1964, p. 831) has shown that most iron-bearing substances considered adequate sources of iron in marine sediments, – e.g., goethite, chlorite, hematite, etc., – will react with H_2S to form iron sulfides when sufficiently fine-grained.

Pyrrhotite is rare in rock salt deposits (Braitsch 1962, p. 18). The mineral is reported only from Aller-Nordstern, Germany (Harbort 1915) and from Morocco (Kosakevitch 1966). In both cases, the pyrrhotite is associated with pyrite.

From Suldrup 15, pyrite is reported from the salt clay/deck halite (Jacobsen 1961). As it has been concluded (Larsen et al. 1961, p. 121) that Suldrup 15 represents different sections (fig. 2B) of the same tectonically disturbed deposit Na2-T3, pyrite most likely also is present in the section represented by fig. 14.

In the Aller-Nordstern deposit, pyrrhotite is observed in halite and kainite ($\text{KCl} \cdot \text{MgSO}_4 \cdot 2.75\text{H}_2\text{O}$) within the carnallite. This paragenesis is altered to kieserite-halite-sylvite-carnallite above 72°C (Braitsch 1962, p. 86). According to Harbort (1915, p. 252), FeCl_2 converts to FeSO_4 , which is reduced to pyrite (FeS_2) by bituminous matter. In the Aller-Nordstern deposit, the reduction proceeded until pyrrhotite formed.

As the concentration of sulphate in the ferruginous metamorphic lye is very low or zero and as the studied pyrrhotite is authigenic, the sulphur may originate from

reduced sulphate of the concentrated sea water, the mother lye (Ulrich et al. 1984, p. 439). However, reduced sulphur and metals may travel in the same solutions under certain conditions concerning high temperature and low pH (Posey and Kyle 1988, p. 20). The reduced sulphur, therefore, may originate from the interval shown at fig. 14.

Optimum temperatures for microbial reduction of sulphate are between 30 and 45°C, and the activity is believed to be reduced drastically at temperatures above 60°C, where the nonmicrobial sulphate reduction by H₂S may be autocatalytic because H₂S is a product of the reaction (Orr 1974, pp. 2313, 2317).

The two other low-temperature magnetic sulfides from anaerobic marine sediments: smythite and greigite (Berner 1964 p. 831–832) are ruled out: smythite, (Fe, Ni)₉S₁₁, has a pseudorhombohedral structure related to that of monoclinic pyrrhotite. Smythite may form secondarily as an oxidation product of monoclinic pyrrhotite at conditions close to room temperature and pressure (Taylor and Williams 1972, p. 1572). Greigite, Fe₃S₄, is a cubic thiospinel (Craig and Scott 1974, p. CS-30).

Brine mixing, salting out

Two types of brine are involved in the formation of the studied halite and fluid inclusions:

- i. a mother lye consisting of concentrated sea water in the NaCl facies, as indicated by the only two solid phases halite and anhydrite. The concentration of CaCl₂ + MgCl₂ is comparatively low, as indicated by the low concentration of CaCl₂ determined by the direct chemical analysis. The ratio CaCl₂: MgCl₂ is unknown but possibly low. The salinity is from ca. 30 to <37 wt.% and the density 1.22–<1.29 g/cm³ (Holser 1979, table 7). The viscosity at 80°C is supposed to be approximately 2 cp (fig. 13).
- ii. A metamorphic lye consisting of the solution resulting from incongruent melting of carnallite (ca. 50 wt.%) and mixed with FeCl₂-rich solutions (ca. 40 wt.%). The mixture proportion is unknown, but the FeCl₂-rich solution must be the minor part, i.e., the salinity of the mixture is 45 wt.% or slightly higher with a density of more than 1.4 g/cm³ (Dietzel 1959, app. 2). The viscosity at 80°C is estimated to 6–8 cp. The grey salt from 1005.5–1029.9 m drilled depth is mineralized with secondary carnallite as scattered grains (fig. 3) and as fracture fillings, increasing downwards. This strongly supports the assumption of infiltrating carnallitic solutions.

The inclusions, regular and irregular, are consanguineous, which means that the concentration differences of the inclusions are caused by differences in brine mixing

of mother lye and metamorphic lye in the original brine pockets. The mother lye is salted out during the mixing (Braitsch 1962, pp. 41–2).

Despite appreciable density, concentration, and especially viscosity disparities (Braitsch 1962, p. 192; Pichavant et al. 1982, p. 24), the salting out of the mother lye was a fast process, as indicated by the large populations of trapped irregular, large inclusions. The salting out is initiated by diffusion (nucleation of NaCl) in the interface zones of the two brines prior mixing (Raup 1970, pp. 2255–6).

At high concentrations of MgCl₂, crystallization of halite is inhibited, causing the brine to become extremely supersaturated. The natural cooling rate within the salt dome is extremely low, markedly reducing material transfer from solution to solid; i.e., reduces both the growth and the nucleation rates (Sarig et al. 1978, p. 666). However, such supersaturated solutions are sensitive to agitation, and the supersaturation may break under the effect of natural turbulence (Karcz and Zak 1987, p. 725).

The resulting brine after mixing and salting out, trapped in the studied inclusions, has a mean concentration of ca. 114 mol MgCl₂ + ca. 2 mol KCl + ca. 2 mol NaCl + 5–10 mol FeCl₂ per 1000 mol H₂O + minor concentrations of CaCl₂ etc., giving a salinity of ca. 40 wt.%. The density is ca. 1.35 g/cm³ or slightly higher, and the viscosity at 80°C is approximately 4 cp.

After the fast salting out, the remaining mixed solution was squeezed out from the former cavity, except for a small amount from which the euhedral crystal of halite (pl. I, fig. 9) slowly crystallized, possibly during the following geologic cooling period.

Temperatures and pressures of formation

The dissolving temperature $T_m = 81.9^\circ\text{C}$ of the grain of carnallite in inclusion no. 27 is a minimum trapping temperature for the inclusion if the carnallite is a daughter mineral; i.e., a minimum crystallization temperature of the studied halite. The recent in situ temperature in Suldrup 15 was not measured. However, the in situ temperature at a depth of 1000 m in the well Erslev 1, Mors dome, was measured to 39°C before complete equilibration. Hence, the in situ temperature is estimated to be ca. 40°C. An in situ temperature of 80°C was measured at a depth of ca. 3400 m (ELK-RAFT and ELSAM 1981, fig. 6.12). Transferred to Suldrup 15, the studied salt crystallized at a depth of 3400 m and was then lifted 2400 m by the postdiapiric movements.

According to Richter-Bernburg (1981, p. 30), the postdiapiric speed of positive salt movements was 0.020–0.025 mm/annum in the Upper Cretaceous and since the Eocene 0.010 mm/annum in the Mors dome.

The postdiapiric movements since the Eocene make

ca. 550 m and in the Upper Cretaceous-Paleocene ca. 1100 m. Consequently, the metamorphic lye infiltrated the studied salt during the end of the diapiric penetration phase at the beginning of the Cretaceous. Tectonic movements during the penetration phase are vigorous, resulting in the disturbances seen in Suldrup 15 (figs. 2B, 14). The disturbances also gave rise to the natural turbulence needed for breaking the supersaturation of the studied mixed brines, combined with the higher pressure of the metamorphic lye coming from lower levels.

The recent lithostatic pressure at a depth of 1000 m in Suldrup 15 is 20–22 MPa, calculated from ca. 165 m overburden of ordinary sediments, ca. 75 m cap-rock of gypsum, ca. 525 m grey salt, and ca. 240 m salt clay and hard salt (Bodenlos 1970, table 1). The gypsum bed corresponds to ca. 45 m anhydrite (Borchert and Muir

1964, table 6). The average contents of anhydrite in the grey salt make 3–5%, so, 45 m anhydrite corresponds to more than 1500 m of dissolved salt (Bodenlos 1970, p. 79). The lithostatic pressure at the site of the studied salt at the beginning of the Cretaceous makes approximately 65 MPa, calculated from some few hundred meters of Triassic and Jurassic sediments (Richter-Bernburg 1961) and ca. 2500 m rock salt. The cap-rock was very thin due to the highly saline environment throughout the Triassic time. Also a part of the anhydrite/gypsum cap-rock dissolved since Triassic times by NaCl solutions in combination with the subsidence. The additional tectonic pressure is unknown, but the tectonic pressure during the final stages of the penetration phase may still be high due to the high velocity of the salt: ~ 0.1 mm/annum (Richter-Bernburg 1981, p. 29).

Conclusions

The study of fluid inclusions in halite by means of microthermometry is impeded or prevented because the wall rock participates in the chemical reactions. Measuring the freezing point depression or phase transitions during freezing runs may be especially difficult or impossible in highly concentrated MgCl_2 solutions because unpredictable amounts of hydrohalite form in combination with the MgCl_2 hydrate transitions. These difficulties may be surmounted if known daughter minerals are present at room temperature and pertinent phase diagrams are available. Measurements of the disappearance temperature of the liquid shrinkage vapour bubble are meaningless if compressed gas is present, as was the case in the present study.

Optical, crystallographic, and chemical (melting) methods help to prove that the main daughter mineral is bischofite, $\text{MgCl}_2 \cdot 6\text{H}_2\text{O}$, reported for the first time from Danish deposits. The minerals sylvite and carnallite are also established with certainty.

The salinity and quantitative composition of the studied solutions are established by measuring the dissolving temperatures of the daughter minerals, combined with the phase diagrams $\text{MgCl}_2\text{-H}_2\text{O}$ and $\text{K}_2\text{Cl}_2\text{-MgCl}_2\text{-H}_2\text{O}$, saturated with NaCl.

The minimum crystallization temperature $T_m = 81.9^\circ\text{C}$ of the studied halite, equalling the dissolving temperature of the daughter carnallite.

The chemical and physical conditions of the equilibrium solution at 80°C just after trapping are described as follows:

Concentrations: approximately 114 mol MgCl_2 + 1 mol K_2Cl_2 + 1 mol Na_2Cl_2 + 5–10 mol FeCl_2 per 1000 mol H_2O + minor concentrations of CaCl_2 etc.;

Salinity: ca. 40 weight% total dissolved solids;

Density: slightly higher than 1.35 g/cm^3 ;

Viscosity: ca. 4 cp;

Pressure during trapping: slightly higher than 65 MPa.

If the true trapping temperature is appreciably higher than 81.9°C , only the trapping pressure and the concentration of NaCl will be markedly higher than noted above, whereas viscosity will be slightly lower.

The following precipitation model of the studied halite is proposed:

The precipitation of halite in former brine pockets is caused by mixing of a mother lye rich in NaCl and a metamorphic lye rich in MgCl_2 . The mother lye consists of concentrated sea water in NaCl facies, trapped in cavities during the precipitation of the grey Na₂ rock salt. The metamorphic lye is a mixture of a carnallitic and a rinneitic solution formed in connection with a potash zone. The resulting metamorphic lye, consisting of approximately 120 mol MgCl_2 + 17 mol K_2Cl_2 + 10 mol FeCl_2 + 4 mol NaCl_2 per 1000 mol H_2O , was squeezed out from the potash zone during the end of the diapiric penetration phase in the beginning of the Cretaceous time. The lye left a trail of disseminated grains and fracture fillings of carnallite all the way from the potash zone to the supposed facies boundary ca. 3 m below the studied brine pockets.

Mixing of the mother and metamorphic lysés was facilitated by tectonic movements and by the higher pressure of the metamorphic lye, despite differences of concentrations and viscosities. During mixing, the studied halite was salted out from the mother lye, whereby many large, irregular inclusions formed, indicating a fast salting out. The temperature was minimum 80°C and the pressure was the lithostatic pressure, ca. 65 MPa, plus an unknown supplementary tectonic pressure.

Most of the mixture which remained after the salting out process was squeezed out from the former brine pockets at later tectonic events.

Pyrrhotite, Fe_{1-x}S , is a very rare mineral in evaporite deposits. Only two occurrences (W. Germany and Morocco) have hitherto been reported in the literature. The delicate, euhedral crystals observed in the halite are authigenic and with a direct relation to the FeCl_2 contents of the metamorphic lye; i.e., the FeCl_2 component is the source of iron. The natural concentration of sulphate in concentrated sea water may be the source of sulphur by reduction with bituminous matter of FeSO_4 .

Acknowledgements

The author is greatly indebted to Fritz Lyngsie Jacobsen (Geological Survey of Denmark) for valuable assistance concerning the interpretation of the potash wells of the Suldrup dome and the procurement of test materials. Troels Laier (Geological Survey of Denmark) is thanked for the important chemical analysis.

The careful and constructive review of Jens Konnerup-Madsen (University of Copenhagen) is greatly appreciated.

The project was funded by the Danish Natural Science Research Council (S.N.F.).

References

- Angell, C.A. and Sare, E.J., 1970: Glass-forming composition regions and glass transition temperatures for aqueous electrolyte solutions. *Chem. Phys.* 52: 1058–1068.
- d'Ans, J., 1933: Die Lösungsgleichgewichte der Systeme der Salze ozeanischer Salzablagerungen. Ackerbau Verlag, Berlin: 254 pp.
- d'Ans, J. and Freund, H.E., 1954: Versuche zur geochemischen Rinneitbildung. *Kali u. Steinsalz*, 6: 3–9.
- d'Ans, J., and Sypiana, G., 1942: Löslichkeiten im System $KCl-MgCl_2-H_2O$ und $NaCl-MgCl_2-H_2O$ bei Temperaturen bis etwa 200°C. *Kalivervandte Salze und Erdöl*. 36: 89–95.
- Armstrong, G., Dunham, K.C., Harvey, C.O., Sabine, P.A. and Waters, W.F., 1951: The paragenesis of sylvine, carnallite, polyhalite, and kieserite in Eskdale borings nos. 3, 4, and 6, northeast Yorkshire. *Min. Mag.* No. 214. 29: 667–689.
- Azizov, A.I., 1979: Distribution and formation of bischofite deposits (in Russian). *Sov. Geol.* No. 8: 115–118.
- Baar, A., 1958: Über Gebirgsverformungen durch bergmännischen Abbau von Kaliflözen bzw. durch chemische Umbildungen von Kaliflözen in geologischer Vergangenheit. *Freib. Forsch.-H.*, A 123: 137–159.
- Berner, R.A., 1964: Stability fields of iron minerals in anaerobic marine sediments. *J. Geol.* 72: 826–834.
- Bodenlos, A.J., 1970: Cap-rock development and salt-stock movement. In: D.H. Kupfer (Editor), *Geology and Technology of Gulf Coast Salt*. Sch. Geosci., LSU: 73–86 c.
- Boeke, E., 1911: Über die Eisensalze in den Kalisalzagerstätten. *Neues Jahrbuch f. Mineral., Geol. u. Paläontologie*: 50–76.
- Borchert, H. and Muir, R., 1964: *Salt Deposits*. D. Van Nostrand Company, Ltd. London: 338 pp.
- Borisenko, A.S., 1978: Study of the salt composition of solutions of gas-liquid inclusions in minerals by the cryometric method. *The Allerton Press Journal Program*: 11–19.
- Braitsch, O., 1962: *Entstehung und Stoffbestand der Salzlagerstätten*. Springer-Verlag, Berlin-Göttingen-Heidelberg: 232 pp.
- Braitsch, O., 1971: *Salt deposits. Their origin and composition*. Springer-Verlag, Berlin-Heidelberg-New York: 297 pp.
- Campbell, A.N., Downes, K.W. and Samis, C.S., 1934: The system $MgCl_2-KCl-MgSO_4-H_2O$ at 100°. *J. Am. Chem. Soc.* 56: 2507–2512.
- Carter, N.L. and Heard, H.C., 1970: Temperature and rate dependent deformation of halite. *Am. J. Sci.* 269: 193–249.
- Craig, J.R. and Scott, S.D., 1979: Sulfide phase equilibria. In: *Sulfide mineralogy* (P.H. Ribbe ed.). *Min. Soc. Am. Short Course Notes*, 1: CSI-CS110.
- Dietzel, H., 1959: Die Dichten im System $MgCl_2-H_2O$ zwischen 20° und 160°C. *Freib. Forsch.-H.*, A132: 21–32.
- Dietzel, H. und Serowy, F., 1959: Die Lösungsgleichgewichte des Systems $MgCl_2-H_2O$ zwischen 20° und 200°C. *Freib. Forsch.-H.*, A132: 1–19.
- Egnsudviklingsrådets boreudvalg, 1962: *Kaliboringerne ved Suldrup. 1959–1961*. København, Vol. I-III.
- ELKRAFT and ELSAM, 1981: *Deponering af højaktivt affald fra danske kernekraftværker. Salthorstundersøgelser*. København. Vol. II.
- Fabricius, J., 1984: Formation temperature and chemistry of brine inclusions in euhedral quartz crystals from Permian salt in the Danish Trough. *Bull. Mineral.*, 107: 203–216.
- Fabricius, J., 1985: Studies of fluid inclusions in halite and euhedral quartz crystals from salt domes in the Norwegian-Danish basin. In: B.C. Schreiber and H.L. Harner (Editors), *Sixth International Symposium on Salt*, Toronto, 1983. The Salt Institute, Alexandria, Virginia, USA, 1: 247–255.
- Fabricius, J., 1987a: Natural Na-K-Mg-Cl solutions and solid derivatives trapped in euhedral quartz from Danish Zechstein salt. In:

- E.E. Horn and H.-J. Behr (Guest-Editors), Current Research on Fluid Inclusions. *Chem. Geol.*, 61: 95–112.
- Fabricius, J., 1987b: Geochemical investigation of potassium-magnesium chloride mineralization of Zechstein 2 salt, Mors dome, Denmark. *DGU. Ser. A. No. 19*: 48 pp.
- Fabricius, J., 1988: Paragenese- og geokemistudier af K-Mg-zoner i det nordjyske Zechstein bassin. *DGU. Ser. D. No. 5*: 94 pp.
- Fabricius, J. and Rose-Hansen, J., 1987: Pressure-dependent melting of carnallite, $\text{KMgCl}_3 \cdot 6\text{H}_2\text{O}$, in a closed system. Contribution to IX. Symposium on Fluid Inclusions, Oporto.
- Findlay, X., 1907: Einführung in die Phasenlehre. Ambrosius Barth, Leipzig.
- Gerlach, H. and Heller, S., 1966: Über künstliche Flüssigkeitseinschlüsse in Steinsalzkrystallen. *Ber. deutsch. Ges. geol. Wiss. B. Miner. Lagerstätten*. 11.2: 195–214.
- Giesel, W., 1968: Kohlensäureausbrüche im Kohlbergbau an der Werra – Grundlagen und Prognosemöglichkeiten. *Kali u. Steinsalz*, 5: 103–108.
- Grube, G. und Bräuning, W., 1938: Über die Entwässerung von Magnesium-Chloridhexahydrat und Carnallit. *Ztschr. Elektrochem.*, 44: 134–143.
- Gussow, W.C., 1970: Heat, the factor in salt rheology. *Geology-Technology Gulf Coast Salt. Sch. Geoscience, LSU*: 125–148.
- Harbort, E., 1915: Über zonar in Steinsalz und Kainit eingewachsene Magnetkieskrystalle aus dem Kalisalzbergwerk Aller-Nordstern. *Kali*, 9: 250–253.
- Haug, R., 1933: Über den tensiometrischen Abbau des Bischofites. *Adolf Remppis, Marbach a. Neckar*: 53 pp.
- Holser, W.T., 1979: Mineralogy of Evaporites. In: R.G. Burns (Editor), *Marine Minerals*, Mineral. Soc. Am. Short Course Notes, Vol. 6: 211–294.
- Jacobsen, F.L., 1961: Mineralogisk-Petrografisk Rapport. Det kerneborede interval 575.00–1084.17 m. Internal report, 44 *DGU*: 31 pp.
- Jacobsen F.L., 1984: Lithostratigraphy of the Zechstein salts in the Norwegian-Danish basin. *DGU series C No. 1, 2*: 7–70.
- Janat'eva, O.K., 1946: Polytherms of solubility of salts in the tropic system $\text{CaCl}_2\text{--MgCl}_2\text{--H}_2\text{O}$ and $\text{CaCl}_2\text{--NaCl--H}_2\text{O}$ (in Russian). *J. appl. Chem.*, 19: 709–722.
- Karcz, I. and Zak, I., 1987: Bedforms in salt deposits of the Dead Sea brines. *J. Sed. Petr.*, 57. 4: 723–735.
- Kokorsch, R., 1960: Zur Kenntnis von Genesis, Metamorphose und Faziesverhältnissen des Stassfurtlagers in Grubenfeld Hildesia-Mathildenhall, Diekholzen bei Hildesheim. *Beih. Geol. Jb.*, 41: 140 pp.
- Kosakevitch, A., 1966: Authigenic pyrrhotite from Souk-el-Arab du Rharb. *Notes Mém. Serv. Géol. Morocco*, 198: 126–127.
- Kühn, R., 1952: Reaktionen zwischen festen, insbesondere ozeanischen Salzen. *Heidelb. Beitr. Mineral. Petrogr.*, 3: 147–168.
- Larsen, G., Jacobsen, F.L. and Jansson, G., 1961: Sammenlignende studier over kaliforekomster i Suldrup salthorsten. In: *Egnsudviklingsrådets boreudvalg*, 1962. I: 115–138.
- Luzhnaya, N.P. and Verescetina, I.P., 1946: Sodium, Calcium and Magnesium Chlorids in Aqueous Solutions of -57° to $+25^\circ$ (Polythermic Solubility). (in Russian). *Journal of applied Chemistry*, 19, No. 7: 723–733.
- Michelsen, O., Saxov, S., Leth, J.A., Andersen, C., Balling, N., Breiner, N., Holm, L., Jensen, K., Kristiansen, J.I., Laier, T., Nygaard, E., Olsen J.C. Poulsen K.D. Priisholm, S., Raade, T.B., Sørensen, T.R. and Wurtz, J. 1981: Kortlægning af potentielle geotermiske reservoirer i Danmark. *DGU serie B nr. 5*: 96 pp.
- Müller, P. und Heymel, W., 1956: Verfahren zur Bestimmung der Gaskonzentrationen des Südhaz- und Werrakalibergbaus. *Bergbautechnik*, 6: 313–318.
- Orr, W.L., 1974: Changes in sulfur content and isotopic ratios of sulfur during petroleum maturation – Study of Big Horn Basin Paleozoic oils. *A.A.P.G. Bull.* 58.11: 2295–2318.
- Pabalan, R.T. and Pitzer, K.S., 1987: Thermodynamics of concentrated electrolyte mixtures and the prediction of mineral solubilities to high temperatures for mixtures in the system $\text{Na-K-Mg-Cl-SO}_4\text{-OH-H}_2\text{O}$. *Geochim. Cosmochim. Acta*, 51: 2429–2443.
- Pichavant, M., Ramboz, C., and Weisbrod, A., 1982: Fluid immiscibility in natural processes: Use and misuse of fluid inclusion data. I., *Chem. Geol.*, 37: 1–27.
- Posey, H.H. and Kyle, J.R., 1988: Fluid-rock interactions in the salt dome environment: an introduction and review. *Chem. Geol.* 74: 1–24.
- Potter II, R.W., 1977: Pressure corrections for fluid-inclusion homogenization temperatures based on the volumetric properties of the system $\text{NaCl-H}_2\text{O}$. *Jour. Research U.S. Geol. Surv.* 5. No. 5: 603–7.
- Ranganathan, V. and Hanor, J.S., 1988: Density-driven groundwater flow near salt domes. *Chem. Geol.* 74: 173–188.
- Raup, O.B., 1970: Brine mixing: an additional mechanism for formation of basin evaporites. *A.A.P.G. Bull.* 54, 12: 2246–2259. 2246–2259.
- Richter-Bernburg, G., 1953: Stratigraphische Gliederung des deutschen Zechsteins. *Z. deutsch. geol. Ges.* 105: 843–854.
- Richter-Bernburg, G., 1961: Geologische Stellungnahme zum Bohrprogramm auf Kalisalze bei Suldrup/Jütland. In: *Egnsudviklingsrådets boreudvalg* 1962, I: 81–114.
- Richter-Bernburg, G., 1981: Geological remarks about the North Jutland Salt Domes in respect on their suitability for radioactive waste disposal. 39 pp. Unpublished.
- Roedder, E., 1963: Studies of fluid inclusions II: Freezing data and their interpretation. *Econ. Geol.*, 58.2: 167–211.
- Roedder, E., 1967: Metastable Superheated Ice in Liquid-Water Inclusions under High Negative Pressure. *Science*, 155, II: 1413–1417.
- Roedder, E., 1971: Metastability in fluid inclusions. *Soc. Mining Geol. Japan, Spec. Issue*, 3: 327–34.
- Roedder, E., 1982: Application of studies of fluid inclusions in salt samples to the problems of nuclear waste storage. *Acta Geologica Polonica*. 32. 1–2: 109–133.
- Roedder, E., 1984: The fluids in salt. *Am. Min.*, 69: 413–439.
- Roedder, E., Belkin, H.E. and Jenks, G., 1978: Fluid inclusions in core samples from Erda no. 9. In: *Geological characterization report, waste isolation pilot plant (WIPP) site, southeastern New Mexico* (D.W. Powers, S.J. Lambert, S.E. Shaffer, L.R. Hill and W.D. Weart, Editors). Vol. II, Chap. 7.6: 7.47–7.69.
- Sarig, S., Eidelman, N., Glasner, A. and Epstein, J.A., 1978: The effect of supersaturation on the crystal characteristics of potassium chloride. *J. app. Chem. Biotechnol.*, 28: 663–667.
- Stewart, F.H., 1951: The petrology of the evaporites of the Eskdale no. 2 boring, east Yorkshire. III. *Min. Mag.*, 2.12: 557–572.
- Sonnenfeld, P., 1984: *Brines and Evaporites*. Academic Press, Inc.: 613 pp.
- Strakhov, N.M., 1962: Principles of Lithogenesis. Vol. 3. (in Russian). Translated 1970, Plenum Publishing Corporation, New York, Vol. 3, Chapter 2.
- Taylor, L.A. and Williams, K.L., 1972: Smythite, $(\text{Fe, Ni})_9\text{S}_{11}$ – a redefinition. *Am. Min.*, 57: 1571–1577.
- Tröger, W.E., 1971: Optische Bestimmung der gesteinsbildende Minerale. Teil 1. E. Schweizerbart'sche Verlagsbuchhandlung. Stuttgart. 188 pp.
- Tuttle, O.F., 1949: Structural petrology of planes of liquid inclusions. *Jour. Geol.*, 57.4: 331–356.
- Ulrich, M.R., Kyle, J.R. and Price, P.E., 1984: Metallic sulfide deposits in the Winnfield salt dome, Louisiana: Evidence for episodic introduction of metalliferous brines during cap rock formation. *Gulf Coast Assoc. Geol. Soc. Trans.*, 34: 435–442.
- Wardlaw, N.C., 1968: Carnallite-Sylvite relationships in the Middle Devonian Prairie Evaporite Formation, Saskatchewan. *Geol. Soc. Am. Bull.*, 79: 1273–1294.
- Zdanovskij A.B. 1949: The use of Secenov's formula on strong electrolyte solutions. *Zh. Obshch. Khim.*, 19.4: 577–592. (in Russian).
- Ziegler, P.A., 1981: Evolution of Sedimentary Basins in North-West Europe. *Petr. Geol. of the Continental Shelf of North-West Europe*. London: 3–39.

PLATE I

- Fig. 1. Cleavage fragment of recrystallized colourless and limpid halite with a broad and a narrow brine channel. Between the two channels, many opaque angular crystals of authigenic pyrrhotite on the same (100) face of the halite are seen. In the narrow channel, two yellow balls (arrows) of supposed limonite (goethite) after rinneite. Visible between the two channels, but at a deeper level, is an assemblage of crystals of anhydrite. Many slightly irregular and a few regular fluid inclusions are seen.*
- Fig. 2. Accidentally opened irregular fluid inclusion in a cleavage piece. The solution was analyzed by means of atomic absorption: 63 mol $MgCl_2$ + 5 mol Na_2Cl_2 + 5 mol K_2Cl_2 + 2 mol $CaCl_2$ per 1000 mol H_2O . Exposed to the atmosphere, the rest of the solution became yellowish, indicating the presence of $FeCl_2$ in solution.*
- Fig. 3. Hexagonal crystals of authigenic pyrrhotite. The surfaces of the crystals are gritty or glossy like gold foil (arrow). At the top of the picture an assemblage of anhydrite.*
- Fig. 4. Cleavage piece of halite showing birefringent lamellae caused by internal stress. Three irregular fluid inclusions with daughter bischofite can be seen.*
- Fig. 5. Fluid inclusion with accidentally trapped hexagonal crystal of pyrrhotite and a yellow ball, possibly limonite after rinneite. A small vapour bubble clings to the yellow ball.*
- Fig. 6. Fluid inclusions with daughter bischofite and three red crystals of hematite (arrows), transported by the metamorphic lye from a potash zone with primary carnallite.*
- Fig. 7. Ligated parts of a former narrow brine channel with daughter bischofite (arrows).*
- Fig. 8. Regular fluid inclusion with the shape of a negative cube modified with the octahedron. No daughter minerals are seen.*
- Fig. 9. Single crystal of halite with very few fluid inclusions. The root end is a glossy cleavage face. It is possible that the crystal formed in the residual solution during the succeeding geologic cooling period.*

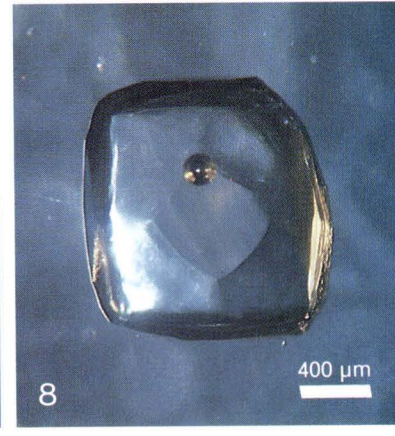
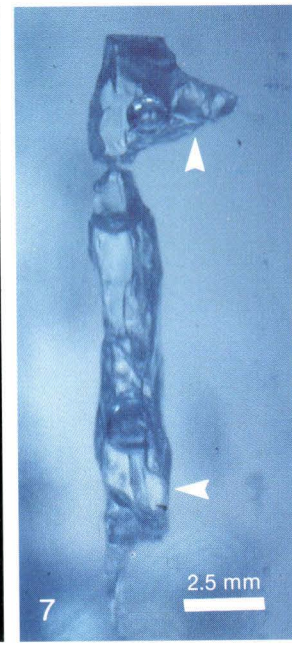
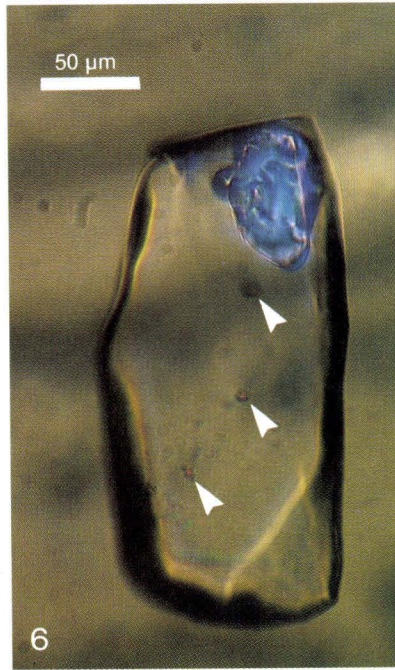
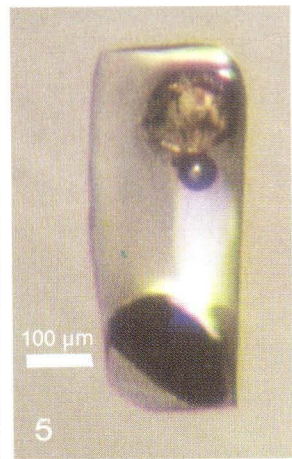
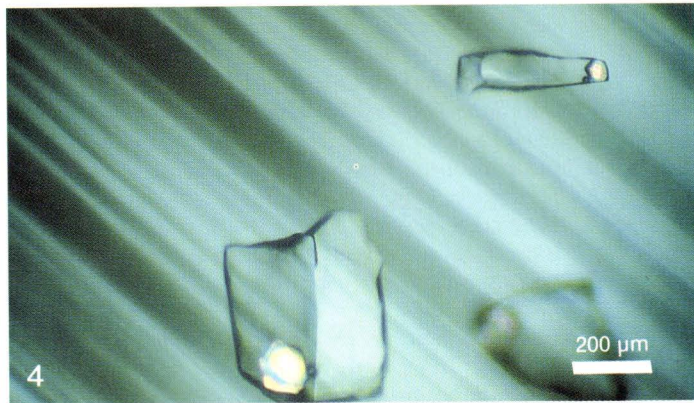
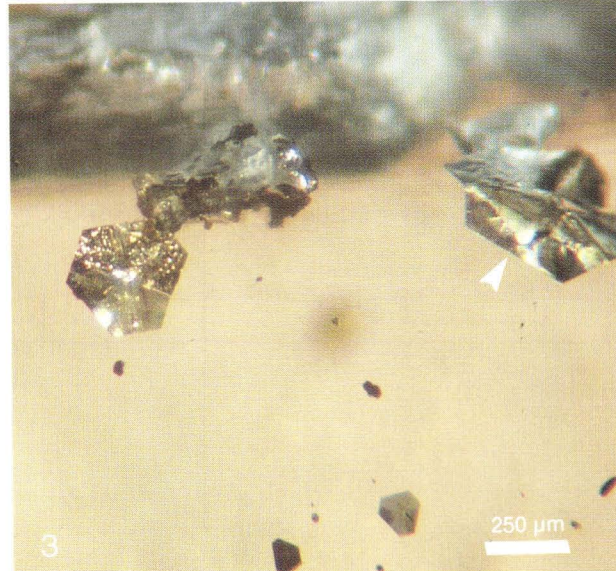
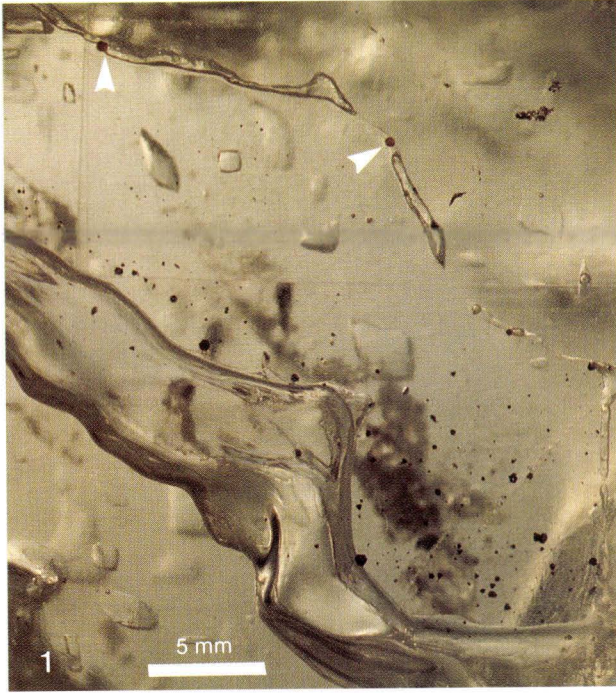


PLATE II

- Figs. 1–4. Pseudo-hexagonal habit of the daughter mineral bischofite. \pm crossed polarisers, gypsum plate. Note the birefringent crystal of ?goethite at fig. 4 (arrow).
- Fig. 5–8. Melting test of bischofite. \pm crossed polarisers, gypsum plate.
- Fig. 5. During a heating run, an inclusion close to the surface of the test sample decrepitated at ca. 170°C. An eruptive vent is piercing the surface (right side of the picture) and numerous droplets of hot brine are thrown out. Through evaporation, the concentration of $MgCl_2$ increases, whereby bischofite crystallizes in the droplets below 100°C. Note the »cinder cone« built up over the vent. The encircled microlite of bischofite is shown at figs. 6–8.
- Fig. 6. During a heating run from room temperature, the microlite suddenly releases water between 50 and 60°C, forming apophyses along its rim.
- Fig. 7. At ca. 110°C, the microlite begins melting. Total melting at ca. 117°C. Fig. 7: 113 – 115°C.
- Fig. 8. After total melting, the test sample was cooled. At ca. 95°C, bischofite suddenly recrystallizes to a few crystallites. During continued cooling, a crystal mush forms.
- Fig. 9. Euhedral bischofite with intergrown triangular crystal of supposed carnallite (red), having a lower dissolving temperature than the host bischofite.
- Fig. 10. Subhedral bischofite with two angular grains of supposed carnallite.
- Fig. 11. Subhedral crystals of carnallite in inclusion no. 27. Note the rough wall of the inclusion. The carnallite dissolved totally at $T_{m,car} = 81.9^\circ C$. The carnallite did not recrystallize during the following cooling to room temperature.
- Fig. 12. After cooling to room temperature, inclusion no. 27 was slowly cooled down to $-45^\circ C$ with no reaction in the solution. During the following warming run, innumerable »Maltese crosses« of isotropic crystals of sylvite formed at ca. $-35^\circ C$. The crosses are arranged on the ceiling of the inclusion in accordance with the crystallography of the host halite.
- Fig. 13. The »Maltese crosses« of fig. 12 start to recrystallize to anisotropic crystals of carnallite ($KCl + MgCl_2$) at ca. $-21^\circ C$, the lower stability limit of carnallite. Many of the crystals of carnallite preserve the original Maltese cross morphology (arrows).

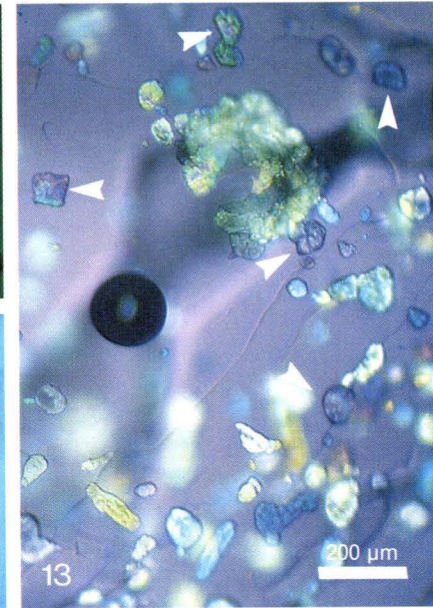
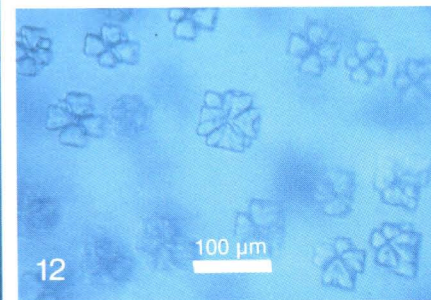
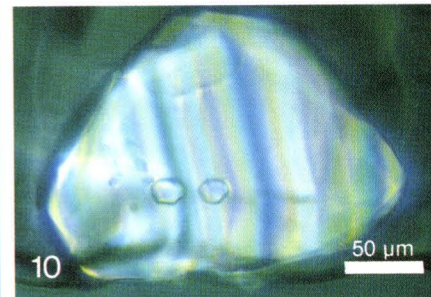
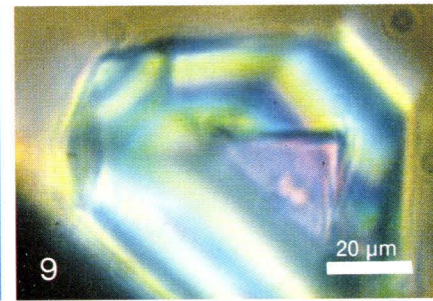
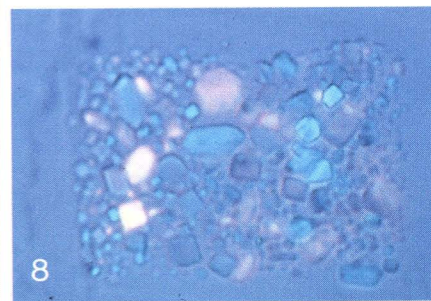
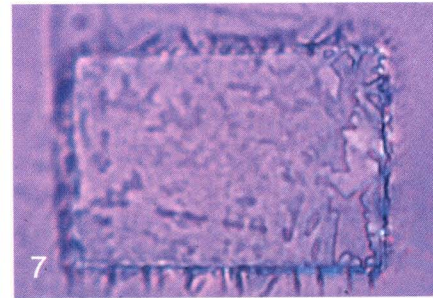
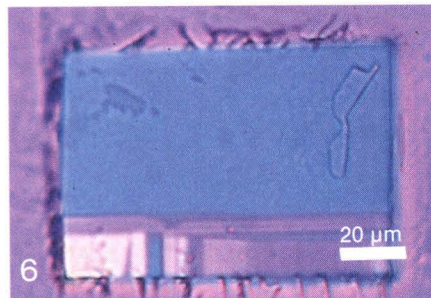
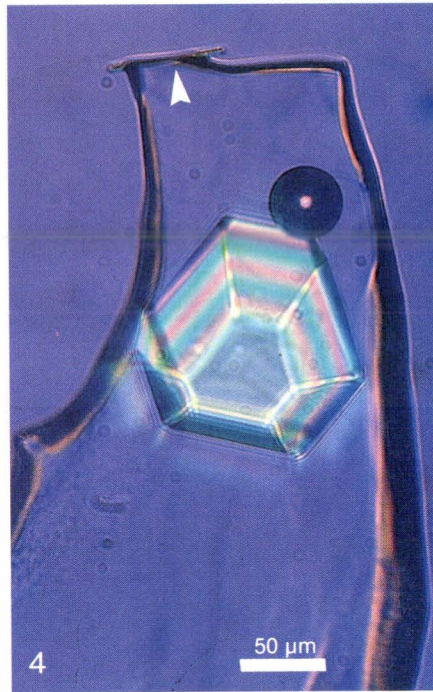
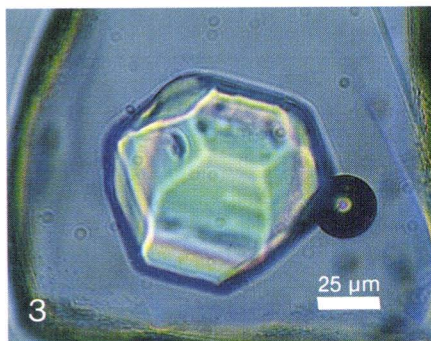
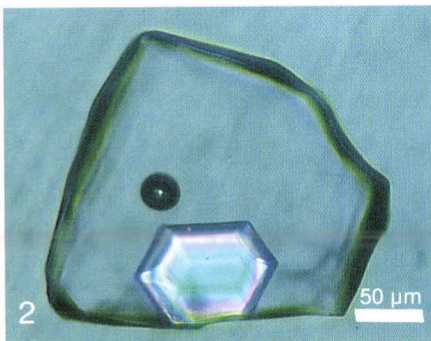
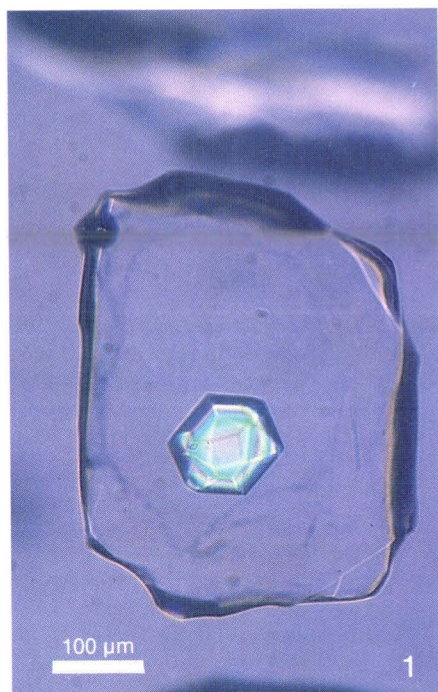
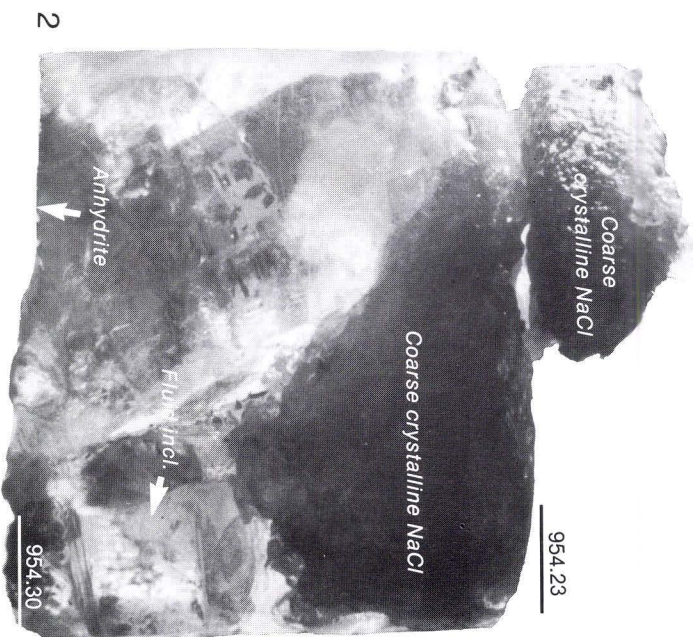
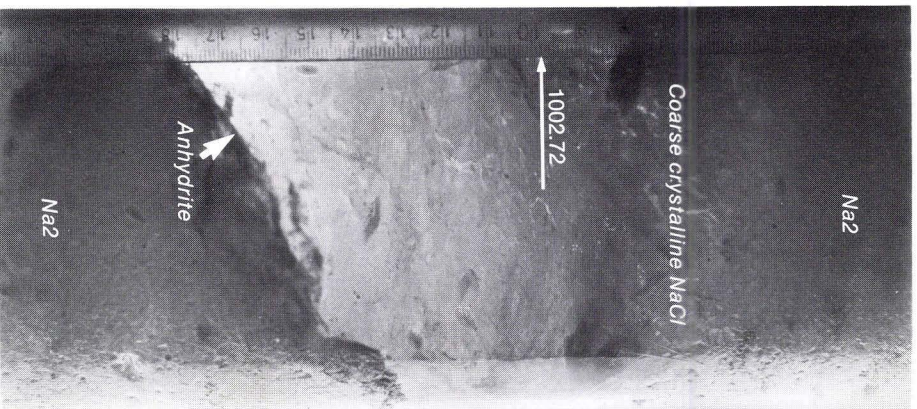


PLATE III

- Fig. 1. Former brine pocket (1002.63 – 1002.75 m, core no 87.15) in typical Na₂ grey rock salt. The brine consists from top of ca. 5 cm coarse crystalline halite (euhedral, limpid crystals, 3–5 mm on an edge) and ca. 7 cm single crystal of halite (colourless and limpid), limited by the core surface. On the base of the pocket a thin medium grey layer (2–4 mm) of minute euhedral crystals of anhydrite forms the transition to the grey salt. F. L. Jacobsen photo (1961).
- Fig. 2. The bottom section of a former brine pocket (954.09 – 954.30 m, core no. 78.10A) in typical Na₂ grey rock salt, consisting of ca. 15 cm coarse crystalline halite (euhedral, limpid, up to 10 mm on an edge) and a large single crystal of halite (colourless and limpid). In the single crystal, a corner (4 × 3 × 3 cm) of a crystal of limpid halite projects from the coarse crystalline layer. No solid inclusions or regular cubic fluid inclusions are observed in the single crystal, whereas highly irregular fluid inclusions with longest dimension up to ca. 15 mm are found here and there. No brine channels, but a couple of empty triangular cavities (longest dimensions ca. 30 mm) are observed along a joint in the crystal. At the base of the single crystal is found a thin layer (1–2 mm) of minute euhedral crystals of anhydrite.
- Fig. 3. Core no. 93.2A (1033.36 – 1033.58 m) consisting of reddish brownish to greyish, partly translucent, coarse to medium grained, heteroblastic rock salt with anhedral reddish brownish crystals (∅ up to 2 cm) of carnallite (arrows). F. L. Jacobsen photo (1961).
- Fig. 4. Core no. 94.12 (1043.28 – 1043.52 m) consisting of greyish with yellowish tint, partly translucent, coarse to medium grained, heteroblastic rock salt with highly irregular grains of colourless to faint violet rinneite (light grey grains). F. L. Jacobsen photo (1961).



Fluid inclusions, trapped in large, limpid cleavages of recrystallized halite from former brine pockets with concentrated sea water, were studied by means of unconventional microthermometry.

The recrystallized halite was salted out from the concentrated sea water by an infiltrating metamorphic lye consisting of a mixture of a carnallitic melt and a rinneitic solution.

The inclusions consist of highly saline K–Mg–Fe–Cl solutions with the daughter mineral bischofite, which is reported from Danish deposits for the first time.

The iron component in the solutions is responsible for the formation of delicate crystals of hexagonal pyrrhotite.